Università degli Studi di Pavia
Dipartimento di Meccanica Strutturale
in collaboration with
Centro di Simulazione Numerica Avanzata – CeSNA
Istituto Universitario di Studi Superiori

A nonlocal cohesive zone model for finite thickness interfaces:

mathematical formulation, numerical implementation and materials science applications

Dr. Ing. Marco Paggi

Politecnico di Torino, Dept. Structural and Geotechnical Engineering

Seminar at the University of Pavia. April 8, 2011, Pavia, Italy

Outline

1. Interfaces in engineering and materials science
2. A nonlocal cohesive zone model (CZM) for finite thickness interfaces based on damage mechanics
3. Interpretation of molecular dynamics (MD) simulations
4. Application to polycrystalline materials
5. Conclusions and future perspectives

M. Paggi, P. Wriggers: "A nonlocal cohesive zone model for finite thickness interfaces – Part I: mathematical formulation and validation with molecular dynamics", **Comp. Mat. Sci.**, Vol. 50 (5), 1625-1633, 2011.

M. Paggi, P. Wriggers: "A nonlocal cohesive zone model for finite thickness interfaces – Part II: FE implementation and application to polycrystalline materials", **Comp. Mat. Sci.**, Vol. 50 (5), 1634-1643, 2011.

Interfaces in forming processes

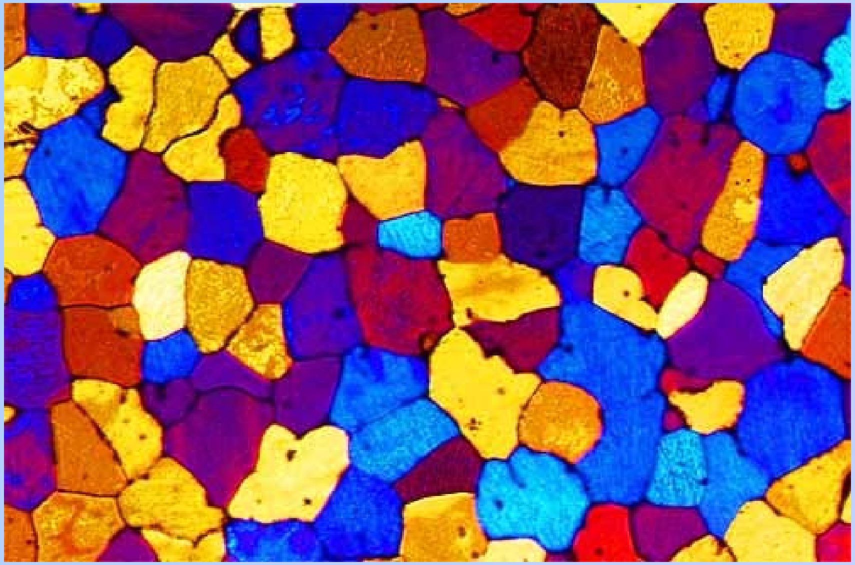

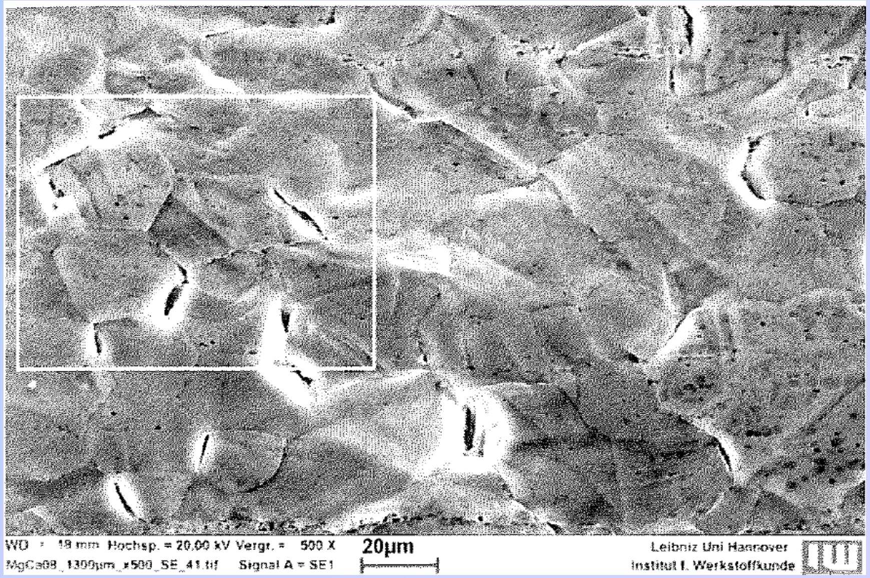

Microcrack formation in CaMg08 (courtesy of Dr. M. Schaper)

P. Kustra, A. Milenin, M. Schaper, A. Gridin: "Multi scale modeling and intepretation of tensile test of Magnesium alloys in microchamber for the SEM", **Computer Methods in Materials Science**, 9:207-214, 2009.

Interfaces in hard-metals for cutting tools

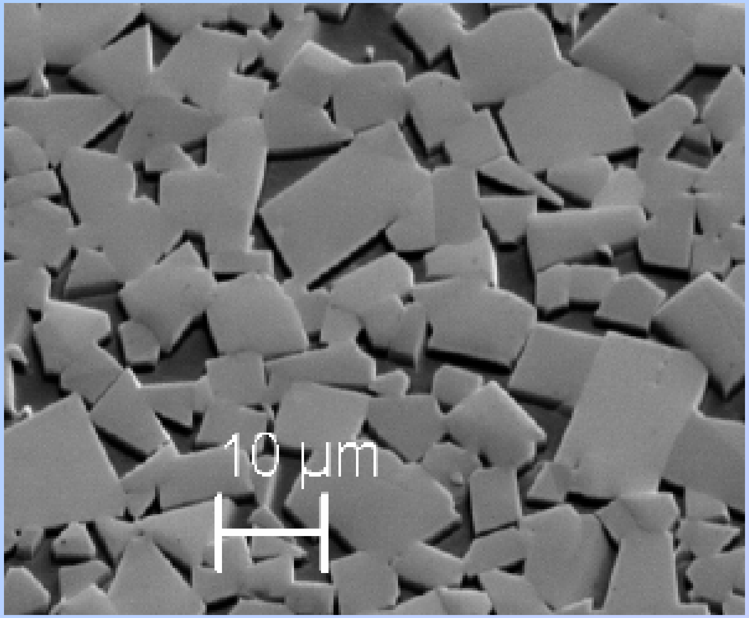

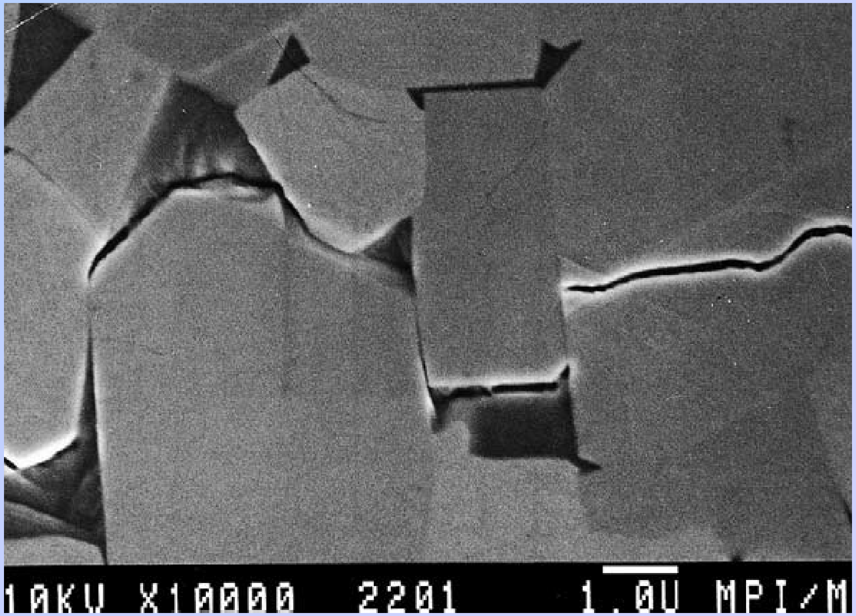

Fracture of a coarse grained WC-10 wt% Co alloy

H. E. Exner, L. Sigl, M. Fripan, O. Pompe: "Fractography of critical and subcritical cracks in hard materials", **Int. J. Refractory Metals and Hard Materials**, 19:329-334, 2001.

Interfaces in solar cells

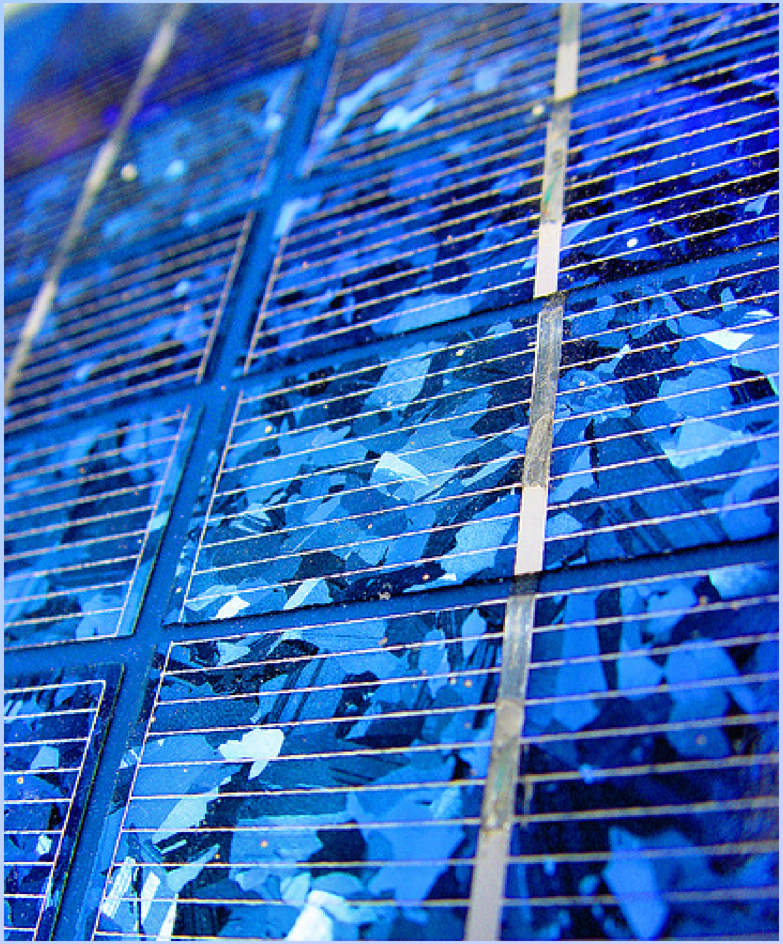

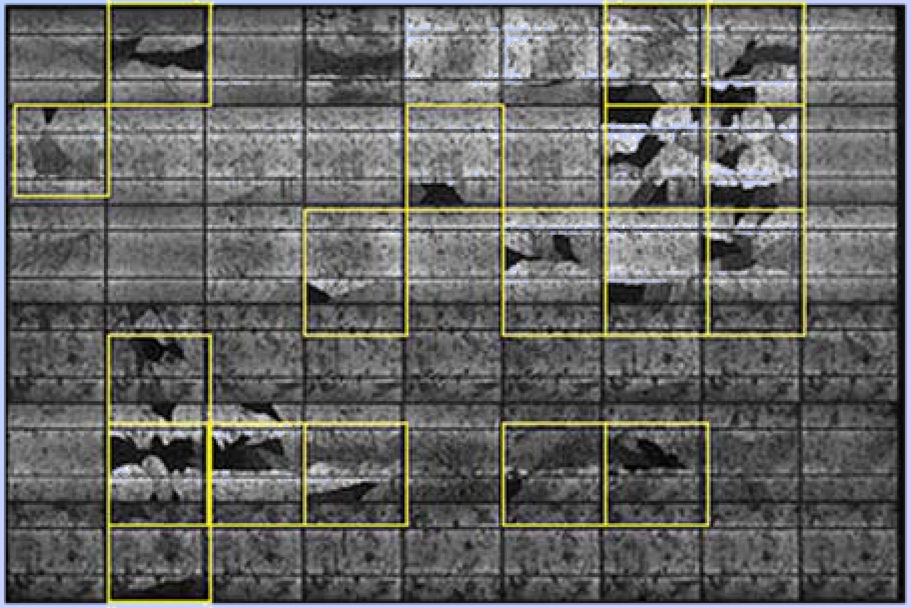

Microcracked photovoltaic modules

Interfaces in hierarchical biological materials

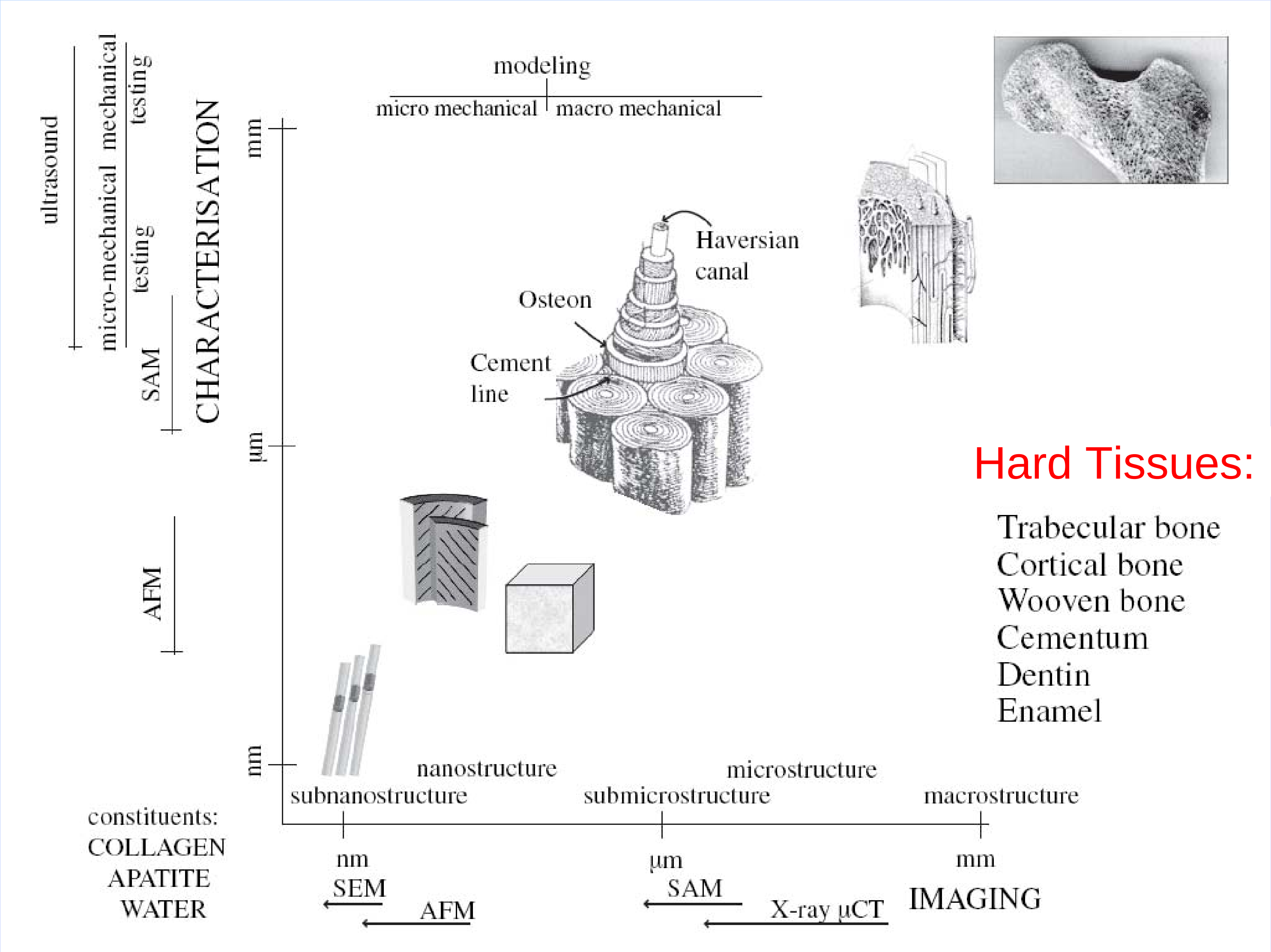

R. De Santis et al.: Ch. 6 in Modeling of Biological Materials, Birkhäuser, Boston, 2007.

Hierarchical polycrystalline materials

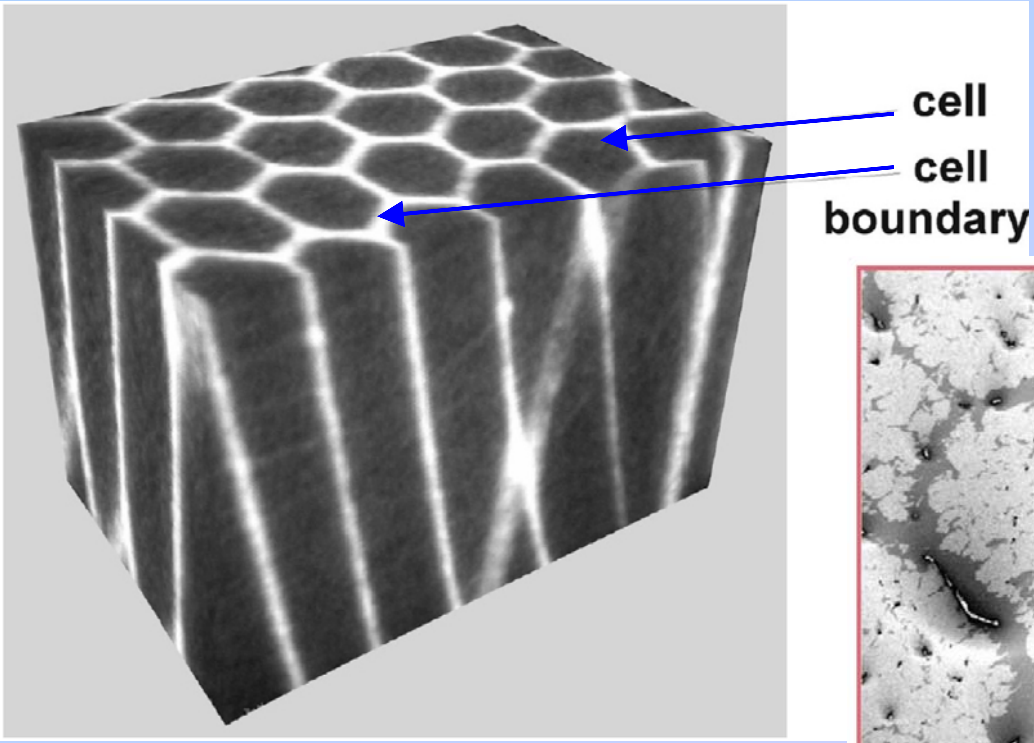

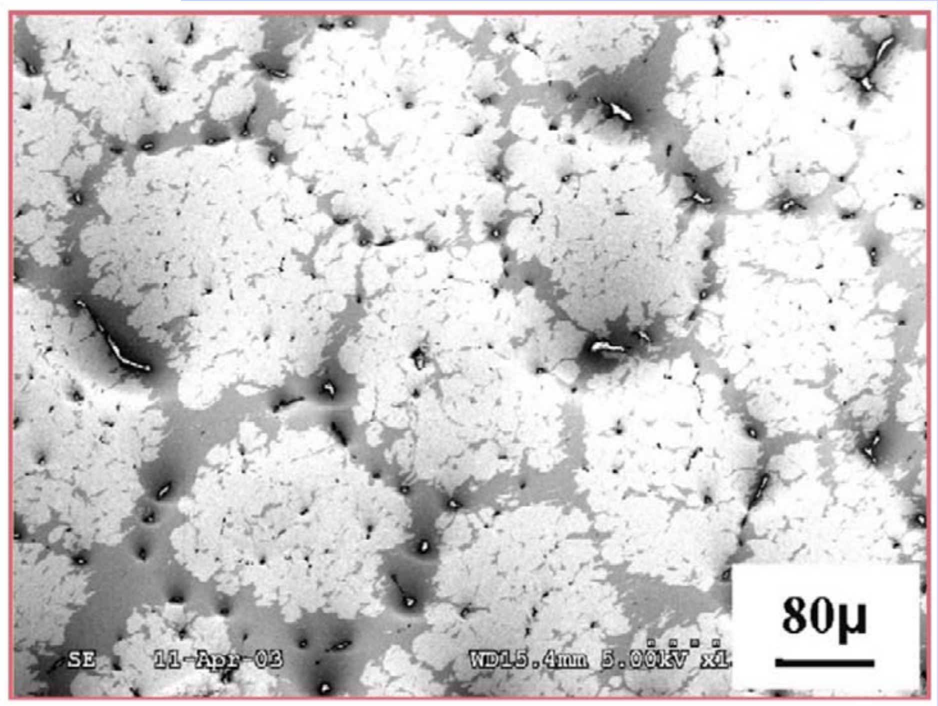

Z.K. Fang et al.: “Fracture resistant super hard materials and hardmetals composite with functionally graded microstructure”, **Int. J. Refr. Metals & Hard Mat.**, 19:453-459, 2001.

Interfaces in engineering

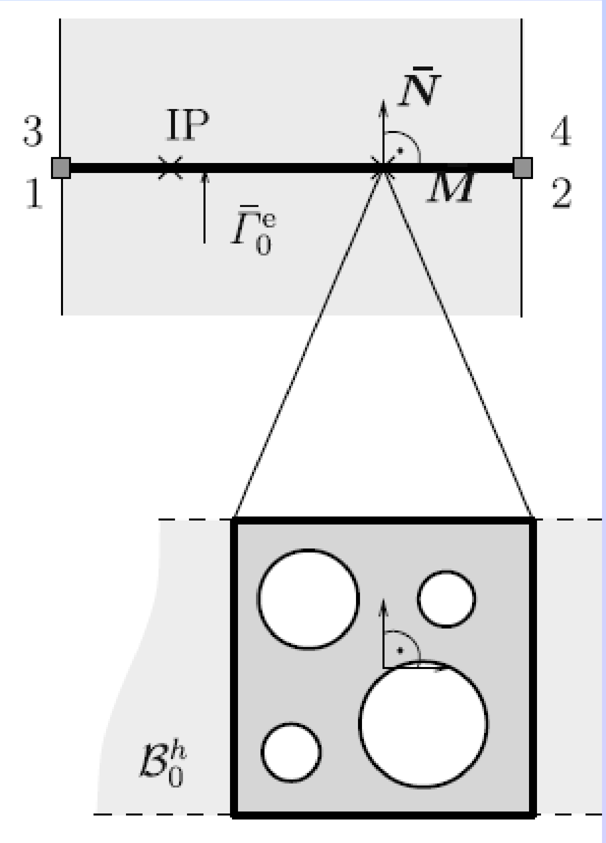

Linking of micro- and macro-scales using the FE^2 method

C.B. Hirschberger, S. Ricker, P. Steinmann, N. Sukumar: "Computational multiscale modelling of heterogeneous material layers", **Engineering Fracture Mechanics**, 76:793-812, 2009.

Interfaces in engineering

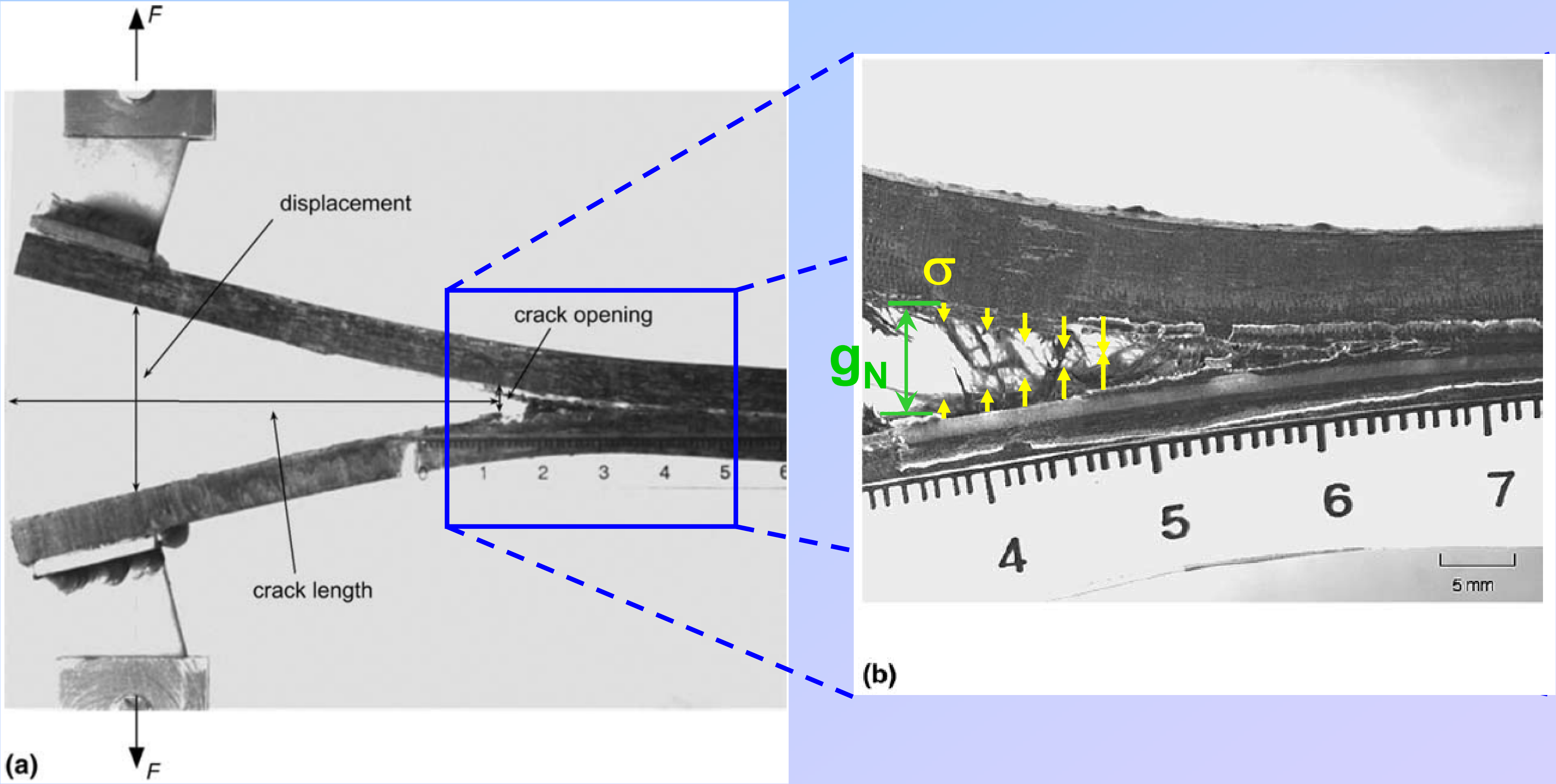

S. Li, M.D. Thouless, A.M. Waas, J.A. Schroeder, P.D. Zavattieri: “Use of mode-I cohesive-zone models to describe the fracture of adhesively-bonded polymer-matrix composite”, **Composites Science and Technology** 65:281-293, 2005.

Cohesive Zone Models (CZMs)

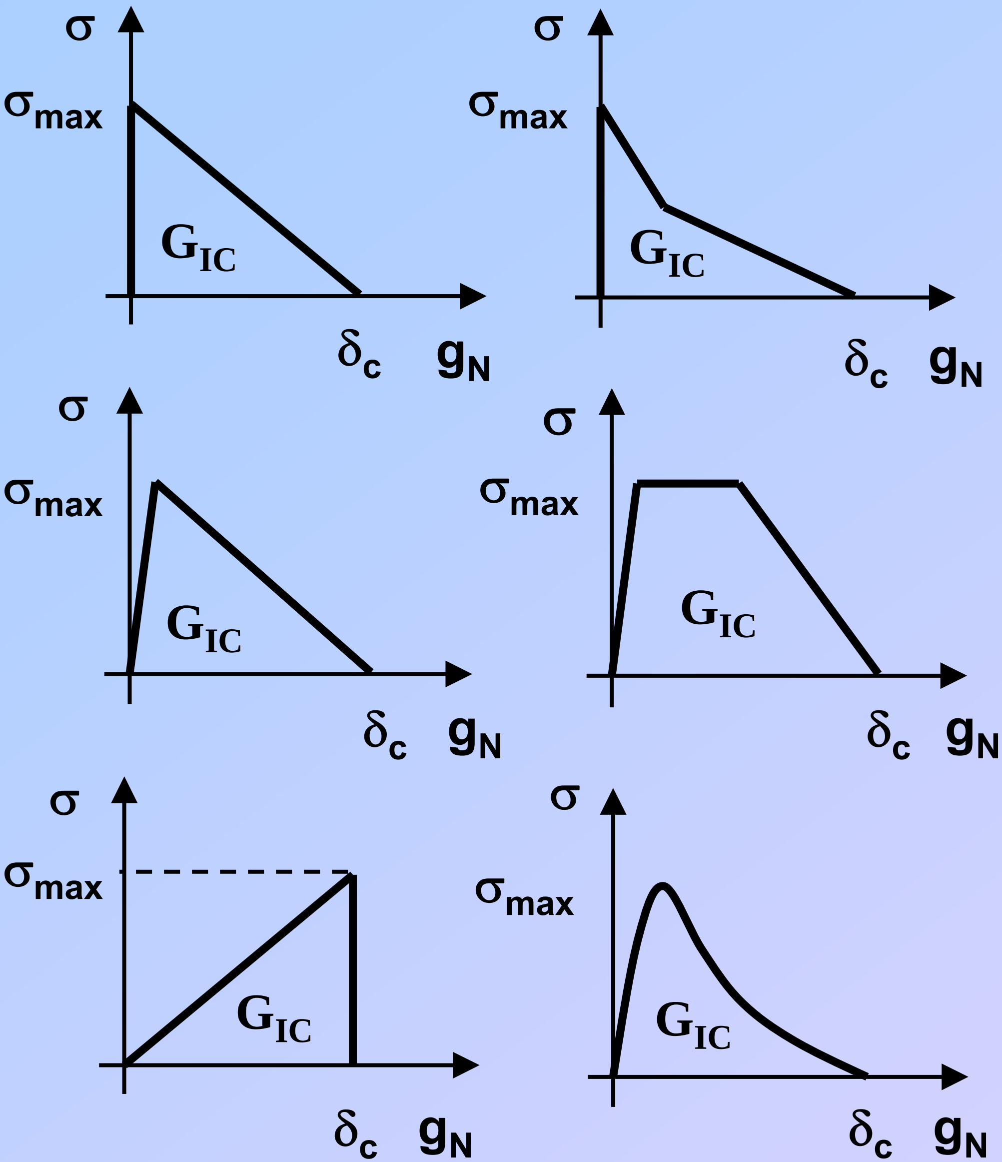

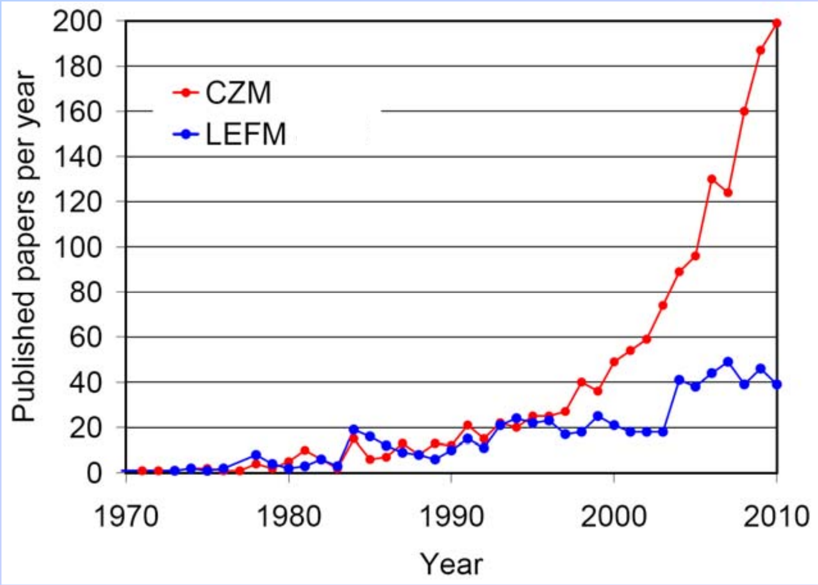

Source: SCOPUS

Open issues:

(1) How to relate the shape of the CZM to physics?

(2) How to take into account the finite thickness properties of real interfaces?

Modelling finite thickness interfaces with DM

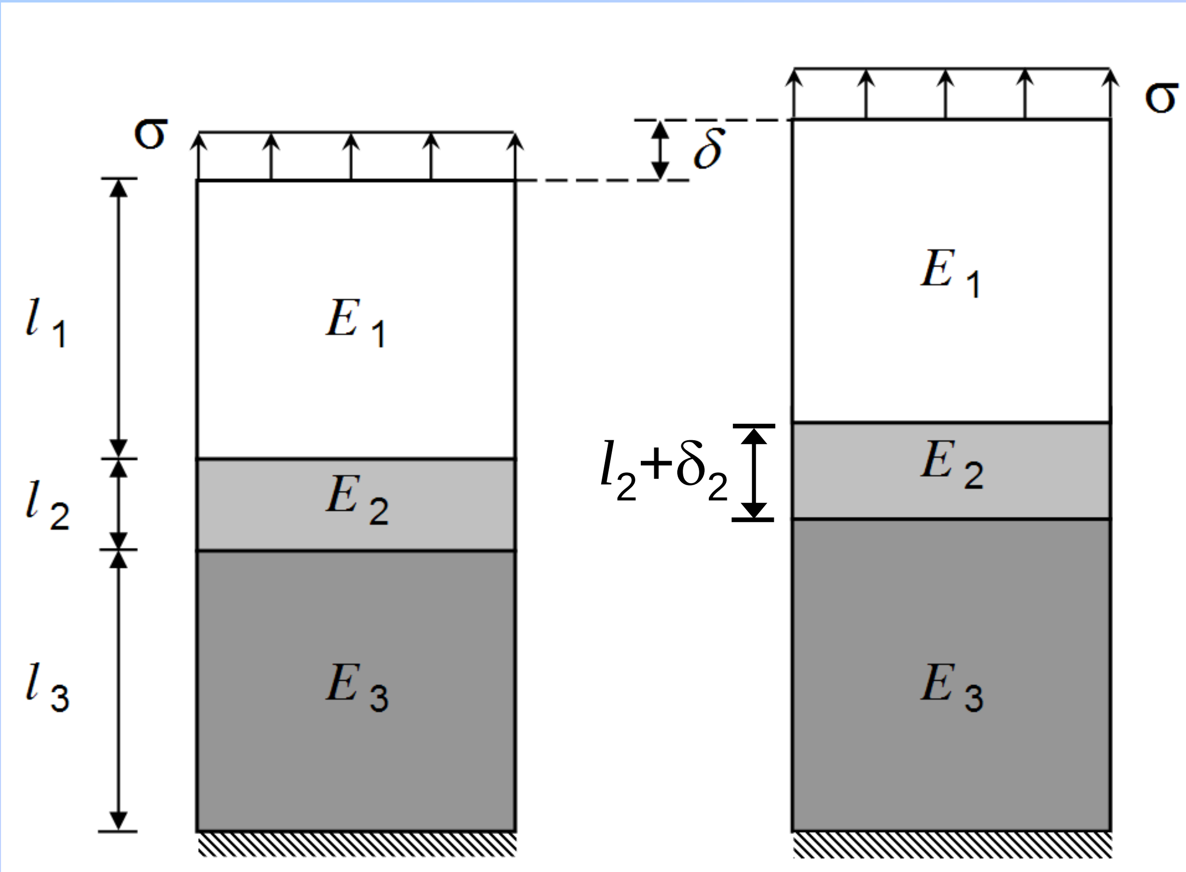

$$E_2 = E_2(1 - D)$$

where damage, *D*, is related to the deformation level of the layer 2:

$$D = \begin{cases} 0 & \text{for} \quad \delta_2 \le \delta_e \\ 1 & \text{for} \quad \delta_2 = \delta_c \end{cases}$$

Modelling finite thickness interfaces with DM

- **1st Stage: all materials behave linear elastically ($0<\delta_2\leq\delta_e$)**

$$\delta = \delta_1 + \delta_2 + \delta_3 = \left(\frac{l_1}{E_1} + \frac{l_2}{E_2} + \frac{l_3}{E_3}\right)\sigma$$

- **2nd Stage: progressive damage in material 2 ($\delta_e<\delta_2<\delta_c$)**

$$\delta = \left[\frac{l_1}{E_1} + \frac{l_2}{E_2(1-D)} + \frac{l_3}{E_3}\right]\sigma$$

- **3rd Stage: failure of the layer 2 ($\delta_2 = \delta_c$)**

$$\sigma = 0$$

Modelling finite thickness interfaces with DM

We put into evidence the increment of axial displacement with respect to the undamaged case:

$$\delta = \left[\frac{l_1}{E_1} + \frac{l_2}{E_2(1-D)} + \frac{l_3}{E_3}\right]\sigma$$

$$\delta = \left(\frac{l_1}{E_1} + \frac{l_2}{E_2} + \frac{l_3}{E_3}\right)\sigma + g_N$$

$$\boxed{g_N = \left[\frac{l_2}{E_2(1-D)} - \frac{l_2}{E_2}\right]\sigma = \frac{l_2 D}{E_2(1-D)}\sigma}$$

Modelling finite thickness interfaces with DM

Damage evolution law

$$D = \left(\frac{w}{w_c}\right)^{\alpha}$$

where

$$\begin{cases} w = (\delta_2 - \delta_e) \\ w_c = (\delta_c - \delta_e) \end{cases}$$

Stress-anelastic displacement relationship, $\sigma = f\,(g_N)$:

$$\boxed{\sigma = \frac{E_2}{l_2} \frac{1 - \left(\frac{w}{w_c}\right)^{\alpha}}{\left(\frac{w}{w_c}\right)^{\alpha}} g_N}$$

where:

$$w = g_N - \delta_e + \sigma l_2 / E_2$$

Analogy with a nonlocal CZM

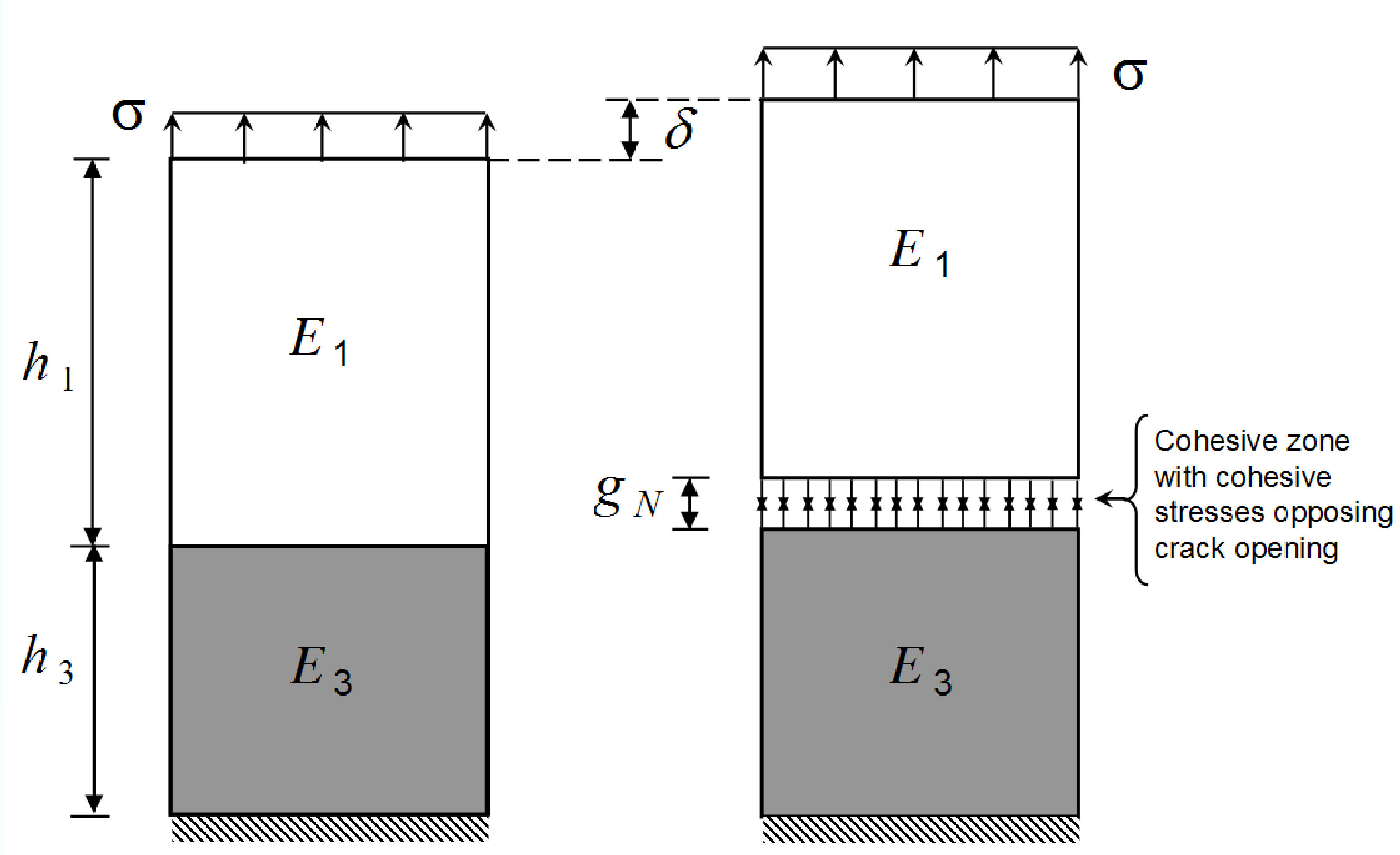

Analogy with a nonlocal CZM

Stage	Trimaterial system with finite thickness interface & DM	Bimaterial system with zero-thickness interface & CZM
1st	$\delta = \left(\frac{l_1}{E_1} + \frac{l_2}{E_2} + \frac{l_3}{E_3} \right) \sigma$	$\delta = \left(\frac{h_1}{E_1} + \frac{h_3}{E_3} \right) \sigma$
2nd	$\delta = \left(\frac{l_1}{E_1} + \frac{l_2}{E_2} + \frac{l_3}{E_3} \right) \sigma + g_N$	$\delta = \left(\frac{h_1}{E_1} + \frac{h_3}{E_3} \right) \sigma + g_N$

A perfect analogy exists if ($h_1+h_3=l_1+l_2+l_3$):

$$h_1 = l_1 + \frac{E_1}{E_2} \left(\frac{E_2 - E_3}{E_1 - E_3} \right) l_2$$

$$h_3 = l_3 + \frac{E_3}{E_2} \left(\frac{E_1 - E_2}{E_1 - E_3} \right) l_2$$

$$g_N = f^{-1}(\sigma) = \frac{l_2 D}{E_2(1 - D)} \sigma$$

Examples in uniaxial tension (Mode I)

Uniaxial tensile test: the effect of the parameter α

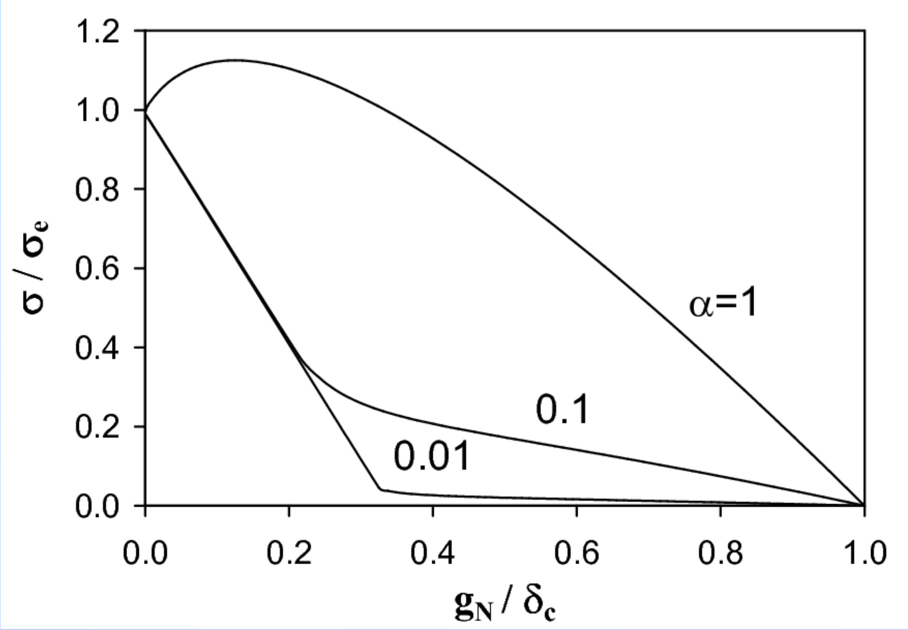

Stress vs. anelastic displacement

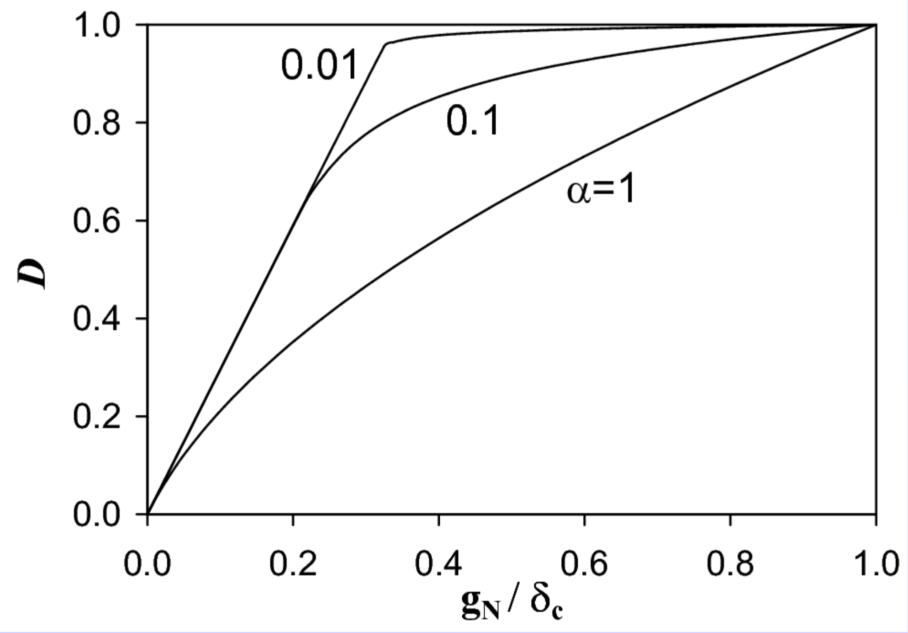

The evolution of damage

Mode II and Mode Mixity

The Mode I model can be generalized by introducing an effective dimensionless opening displacement:

$$\lambda = \sqrt{\left(\frac{w}{w_c}\right)^2 + \left(\frac{u}{u_c}\right)^2}, \quad \lambda \leq 1$$

and

$$D = \lambda^\alpha$$

$$\frac{\sigma}{\sigma_e} = \frac{1-\lambda^\alpha}{\lambda^\alpha} k_N \frac{g_N}{\delta_c}$$

$$\frac{\tau}{\tau_e} = \frac{1-\lambda^\alpha}{\lambda^\alpha} k_T \frac{g_T}{\psi_c}$$

Mode II and Mode Mixity

α=0.1 **α=1.0**

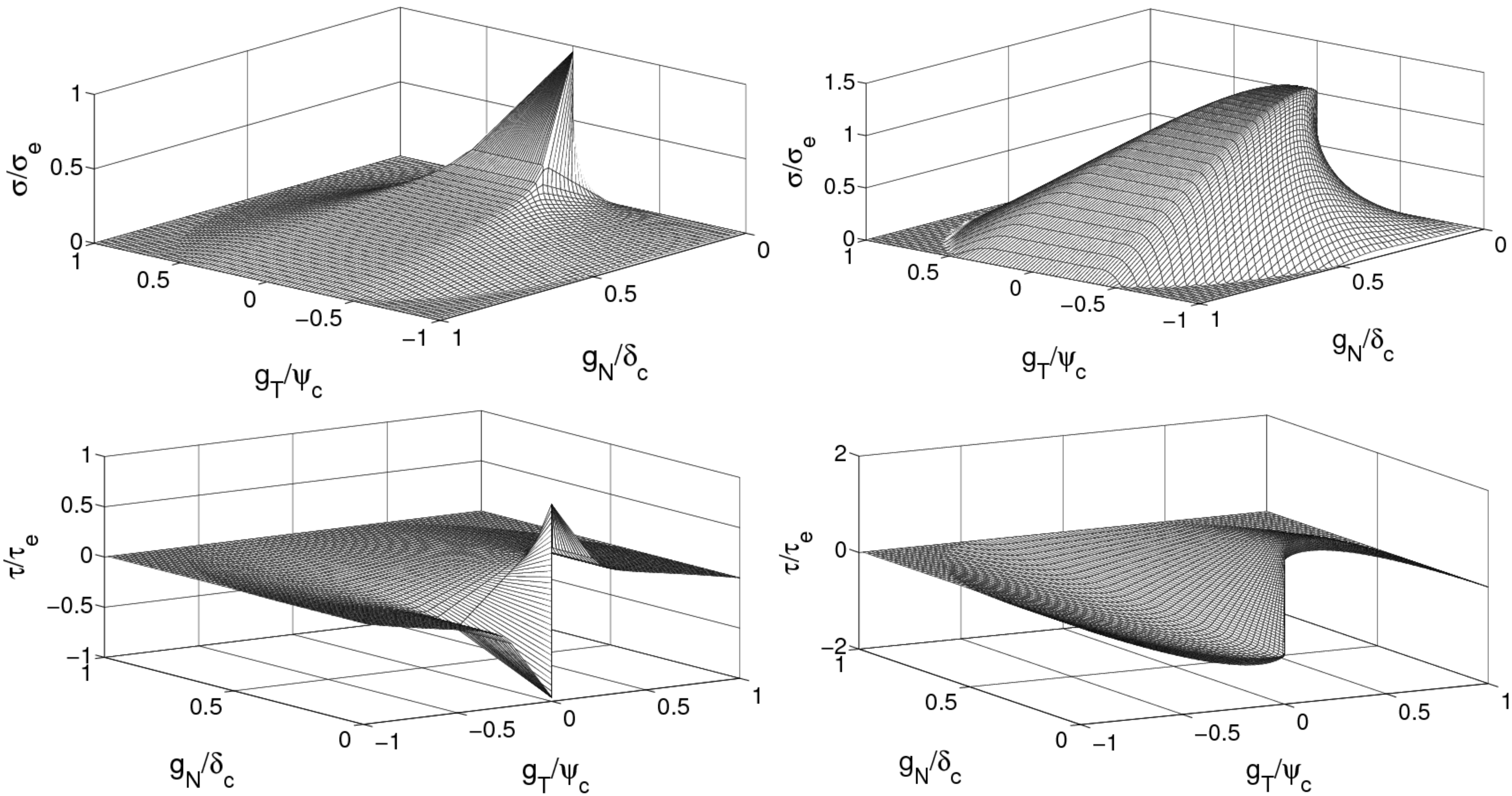

Interpretation of MD simulations

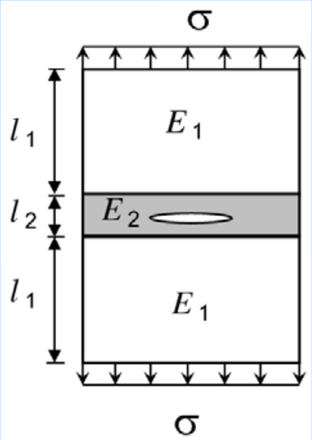

Zhou et al., **Mech. Mater.**, 40:832-845, 2008

Tungsten (bcc crystal)

l_2=3 Å, E_1=384 GPa, E_2=9 GPa

δ_e=0.1 Å, δ_c=9.0 Å, α=0.2

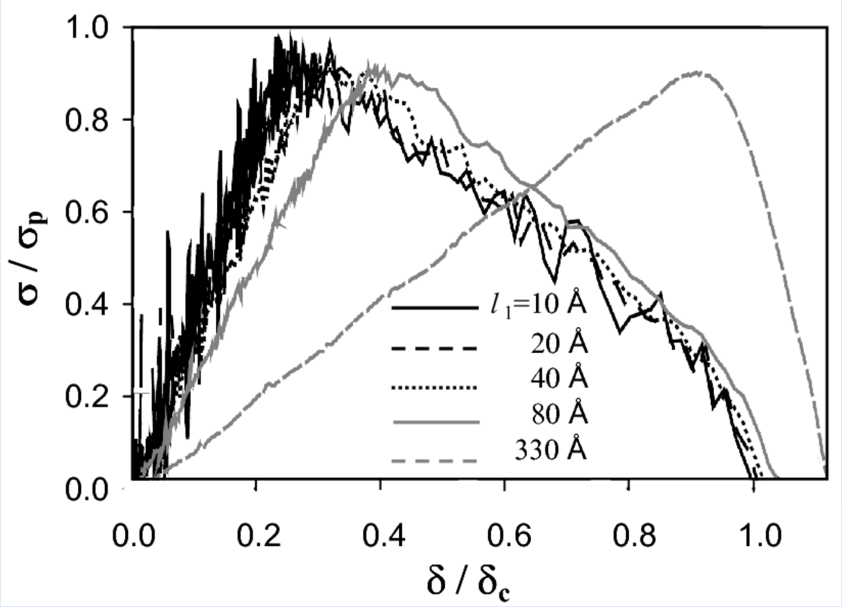

MD results

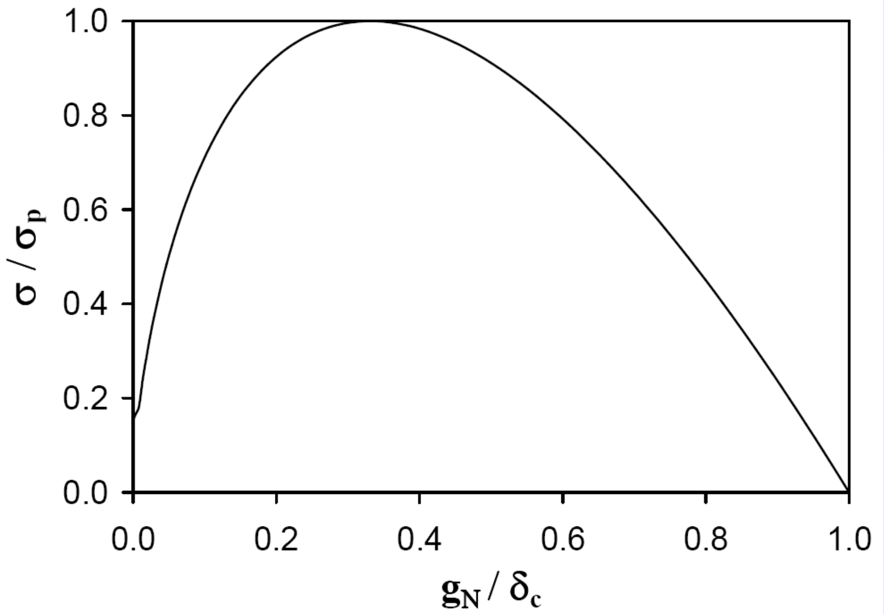

Nonlocal CZM

Interpretation of MD simulations

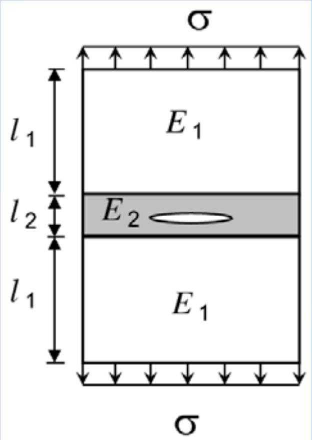

Zhou et al., **Mech. Mater.**, 40:832-845, 2008

Tungsten (bcc crystal)

l_2=3 Å, E_1=384 GPa, E_2=9 GPa

δ_e=0.1 Å, δ_c=9.0 Å, α=0.2

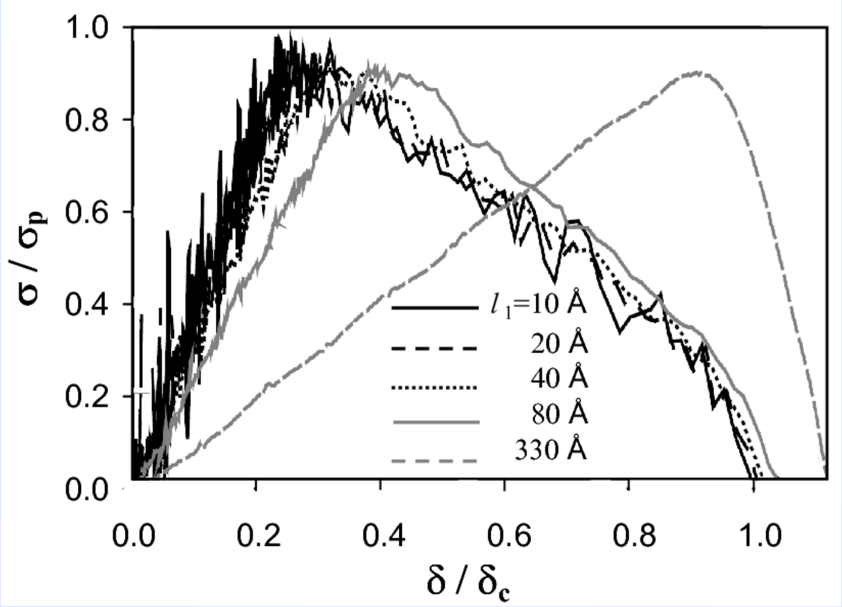

MD results

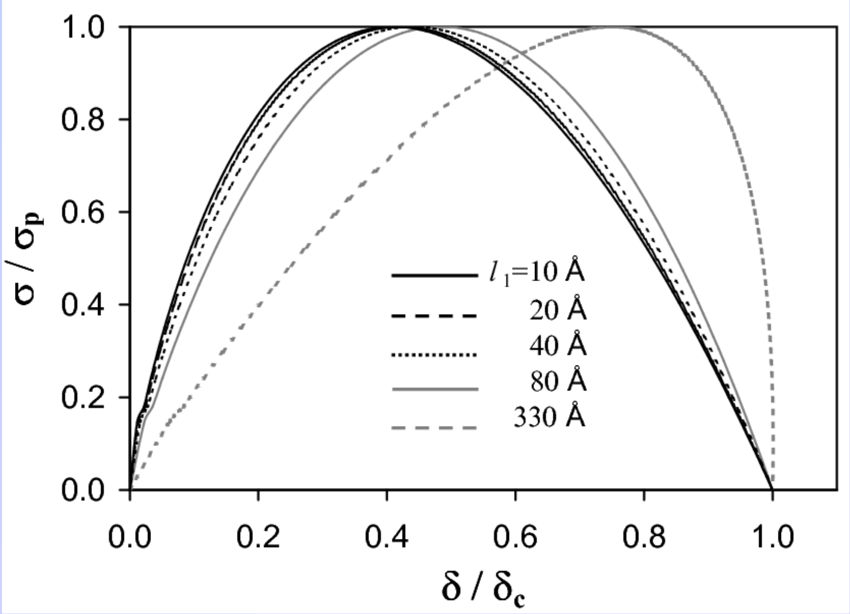

Nonlocal CZM predictions

Interpretation of MD simulations

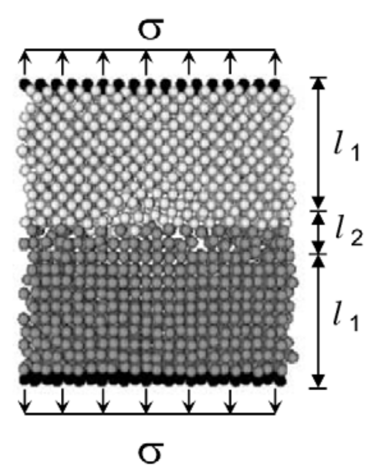

Spearot et al., **Mech. Mater.**, 36:825-847, 2004

Copper (fcc crystal)

$2l_2+l_1$=43.38 Å, $E_1=E_2$=110 GPa

δ_e=0.2 Å, δ_c=8.0 Å, α=0.9

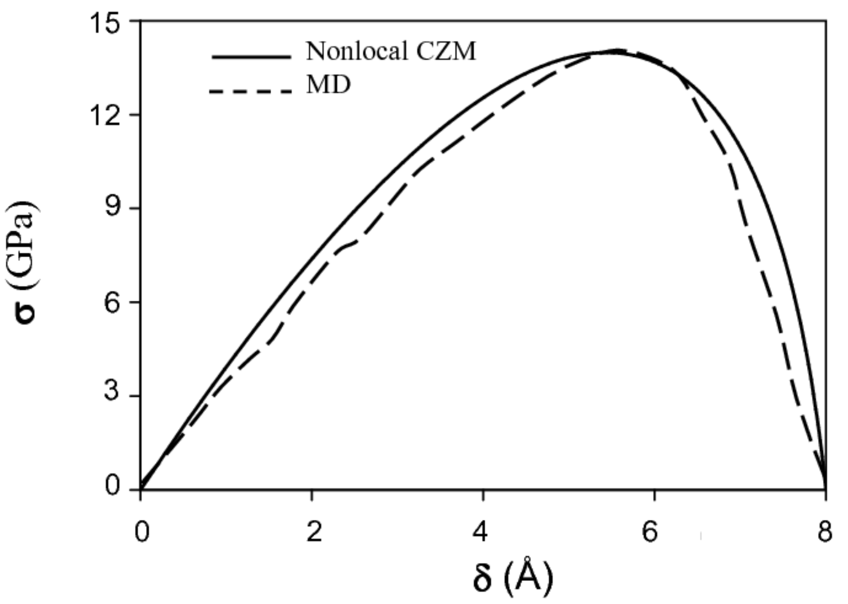

MD-nonlocal CZM comparison

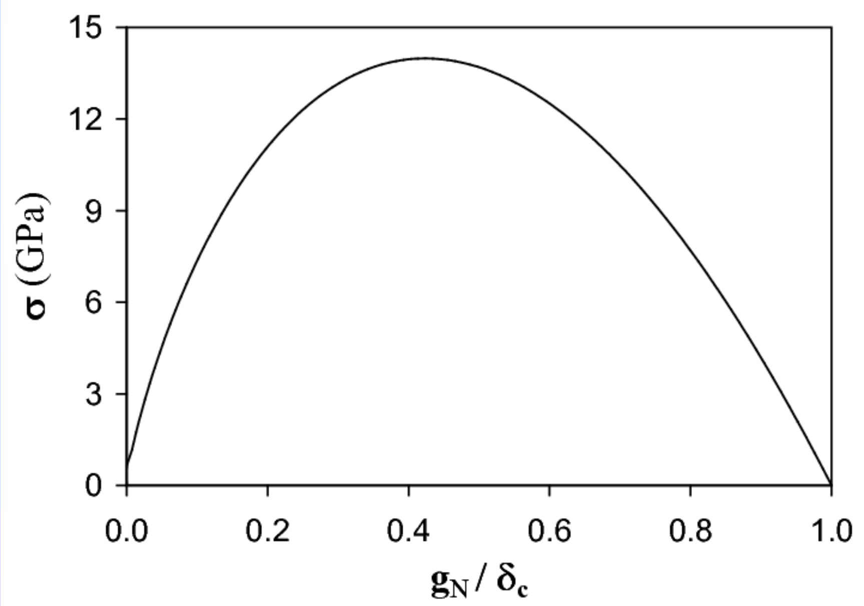

Shape of the nonlocal CZM

Interpretation of MD simulations

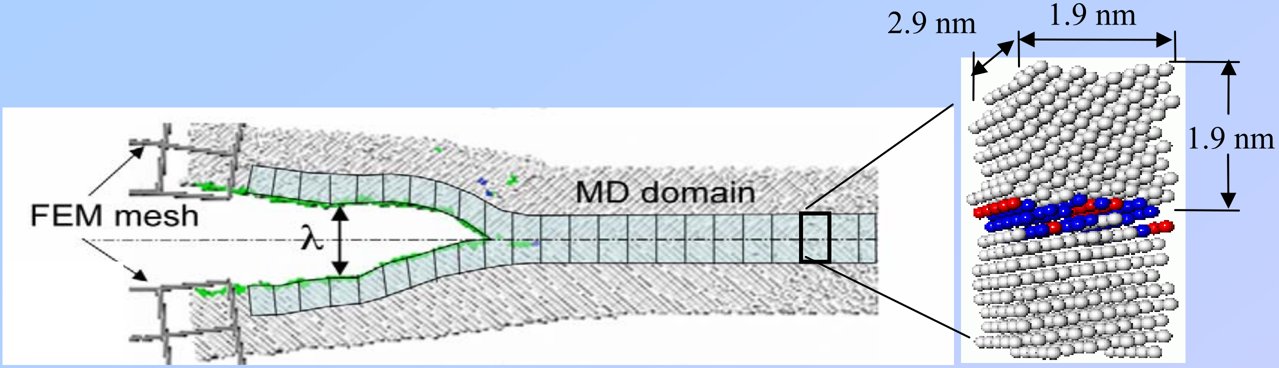

Yamakov et al., **JMPS**, 54:1899-1928, 2006

Aluminum, α=0.05

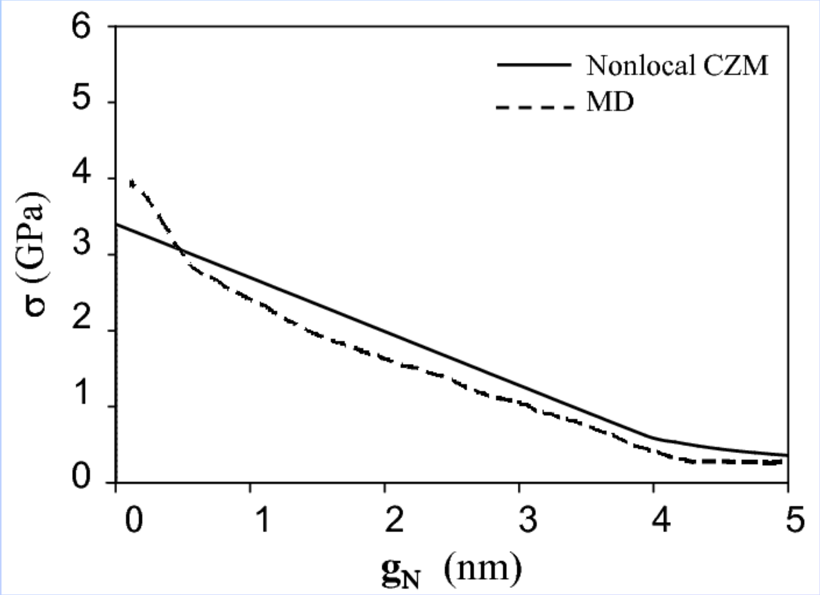

Twinning mechanism

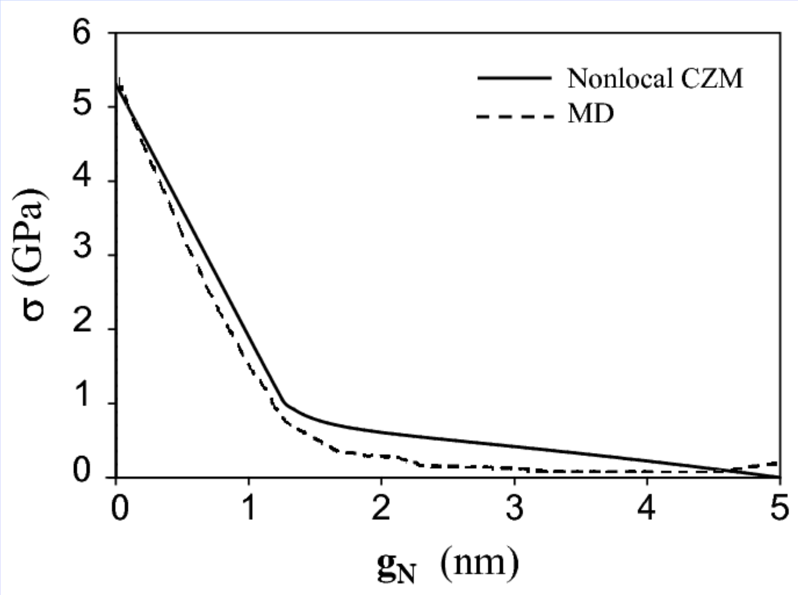

Cleavage mechanism

FE implementation of the nonlocal CZM

$$\mathbf{u} = (u_1, v_1, u_2, v_2, u_3, v_3, u_4, v_4)^{\mathrm{T}}$$

$$\mathbf{u}^* = \mathbf{R}\mathbf{u}$$

$$\Delta\mathbf{u}^* = (u_4^* - u_1^*, v_4^* - v_1^*, u_3^* - u_2^*, v_3^* - v_2^*)^{\mathrm{T}} \quad \Longrightarrow \quad \Delta\mathbf{u}^* = \mathbf{L}\mathbf{u}^*$$

$$\mathbf{g} = \mathbf{N}\Delta\mathbf{u}^*$$

$$\mathbf{g} = \mathbf{NLRu} = \mathbf{BRu}$$

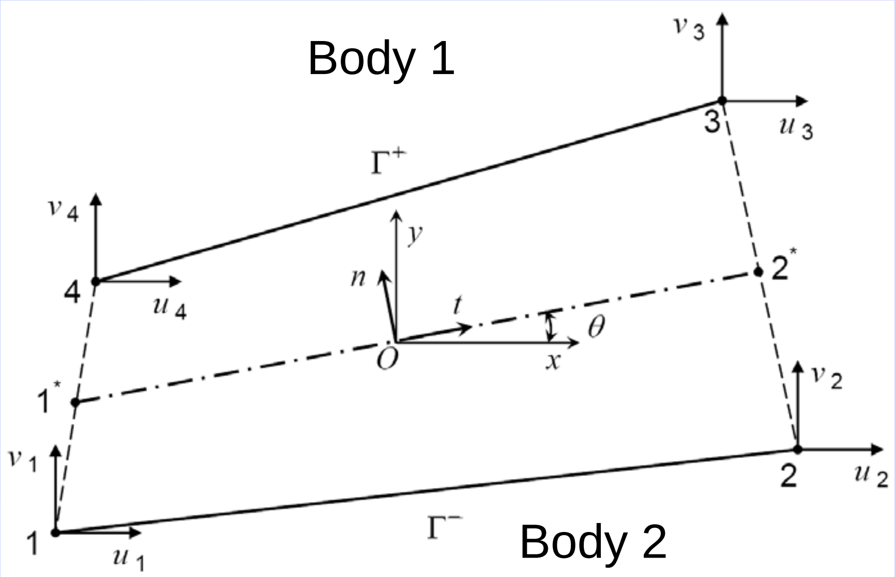

M. Ortiz and A. Pandolfi: “Finite-deformation irreversible cohesive elements for three-dimensional crack propagation analysis”, **IJNME**, 44:1267-1282, 1999.

FE implementation of the nonlocal CZM

$$G_{int} = \int_S \delta \mathbf{g}^{\mathrm{T}} \mathbf{t} \, \mathrm{d}S = \delta \mathbf{u}^{\mathrm{T}} \mathbf{R}^{\mathrm{T}} \int_S \mathbf{B}^{\mathrm{T}} \mathbf{t} \, \mathrm{d}S$$

$$\mathbf{t} = (\tau, \sigma)^{\mathrm{T}}$$

$$\Delta G_{int} = \delta \mathbf{u}^{\mathrm{T}} \mathbf{R}^{\mathrm{T}} \int_S \mathbf{B}^{\mathrm{T}} \mathbf{C} \mathbf{B} \, \mathrm{d}S \mathbf{R} \mathbf{u}$$

$$\mathbf{t} = \mathbf{C}\mathbf{g} = \mathbf{C}\mathbf{B}\mathbf{R}\mathbf{u}$$

$$\mathbf{C} = \begin{bmatrix} \frac{\partial \tau}{\partial g_T} & \frac{\partial \tau}{\partial g_N} \\ \frac{\partial \sigma}{\partial g_T} & \frac{\partial \sigma}{\partial g_N} \end{bmatrix}$$

Residual vector and tangent stiffness matrix:

$$\mathbf{F} = \mathbf{R}^{\mathrm{T}} \sum_{ip=1}^{2} \mathbf{B}_{ip}^{\mathrm{T}} \mathbf{t}_{ip} l/2$$

$$\mathbf{K} = \mathbf{R}^{\mathrm{T}} \left(\sum_{ip=1}^{2} \mathbf{B}_{ip}^{\mathrm{T}} \mathbf{C}_{ip} \mathbf{B}_{ip} l/2 \right) \mathbf{R}$$

Newton-Raphson loop for the computation of t and C

$$\boxed{\begin{aligned}\tau &= \tau_e \frac{1-\lambda^\alpha}{\lambda^\alpha}\frac{g_T}{\psi_e}\\ \sigma &= \sigma_e \frac{1-\lambda^\alpha}{\lambda^\alpha}\frac{g_N}{\delta_e}\end{aligned}}$$

$$\lambda = \sqrt{\left(\frac{w}{w_c}\right)^2 + \left(\frac{u}{u_c}\right)^2}$$

$$w = g_N - \delta_e + \sigma\frac{l_2}{E_2}$$

$$u = g_T - \psi_e + \tau\frac{l_2}{G_2}$$

$$\mathbf{R}^i = \mathbb{I}\,\mathbf{t}^i - \mathbf{r}^i(\mathbf{t}^i) = \mathbf{0}$$

$$\Longrightarrow$$

$$\mathbf{A}^i \Delta\mathbf{t}^{i+1} = -\mathbf{R}^i,$$

$$\mathbf{t}^{i+1} = \mathbf{t}^i + \Delta\mathbf{t}^{i+1}$$

$$\mathbf{C} = -\mathbf{A}\begin{bmatrix}\dfrac{G_2}{l_2} & 0\\ 0 & \dfrac{E_2}{l_2}\end{bmatrix} + \begin{bmatrix}\dfrac{G_2}{l_2}+\dfrac{\tau}{g_T} & 0\\ 0 & \dfrac{E_2}{l_2}+\dfrac{\sigma}{g_N}\end{bmatrix}$$

Convergence of the proposed algorithm

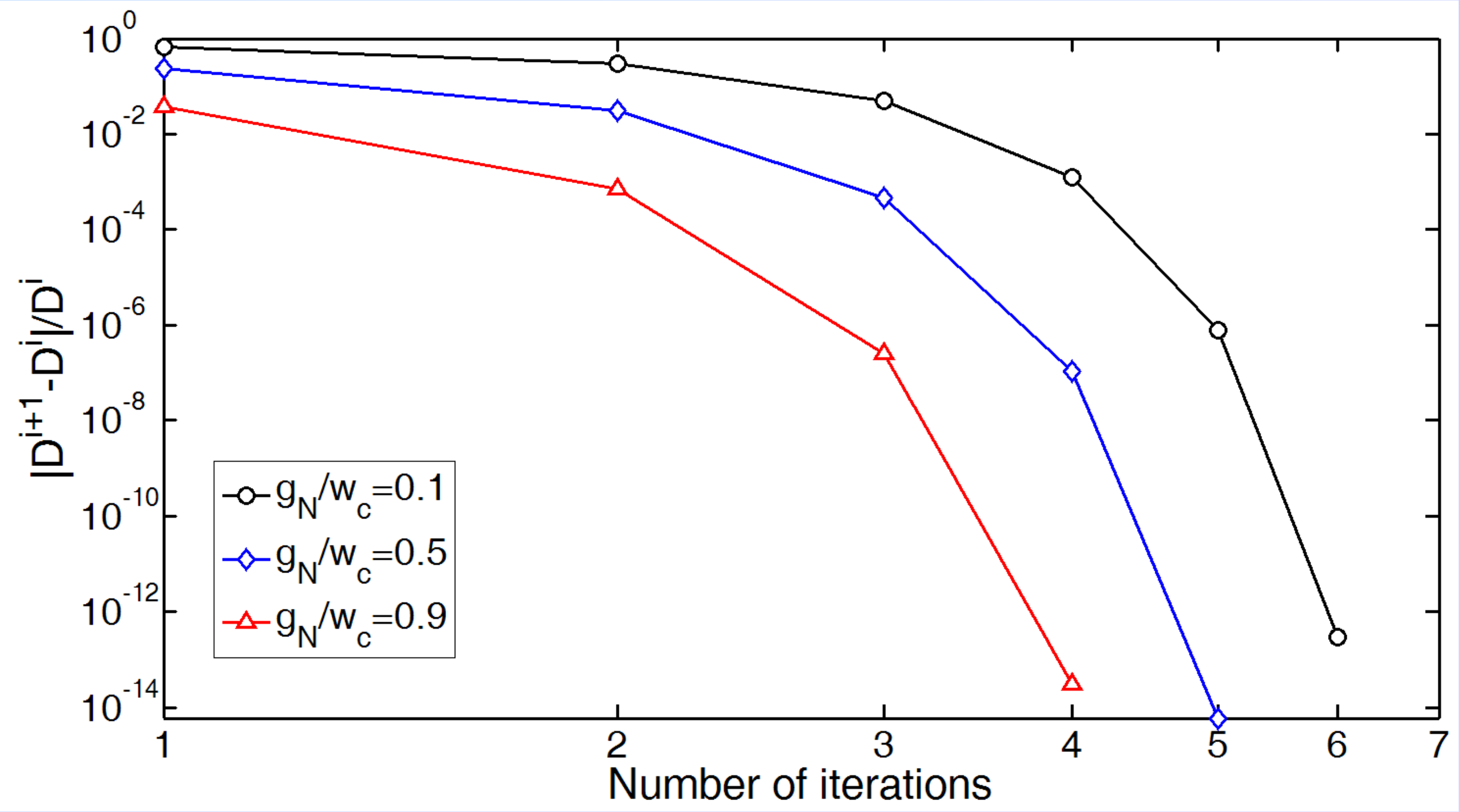

Quadratic convergence of the nested Newton-Raphson loop

Convergence of the proposed algorithm

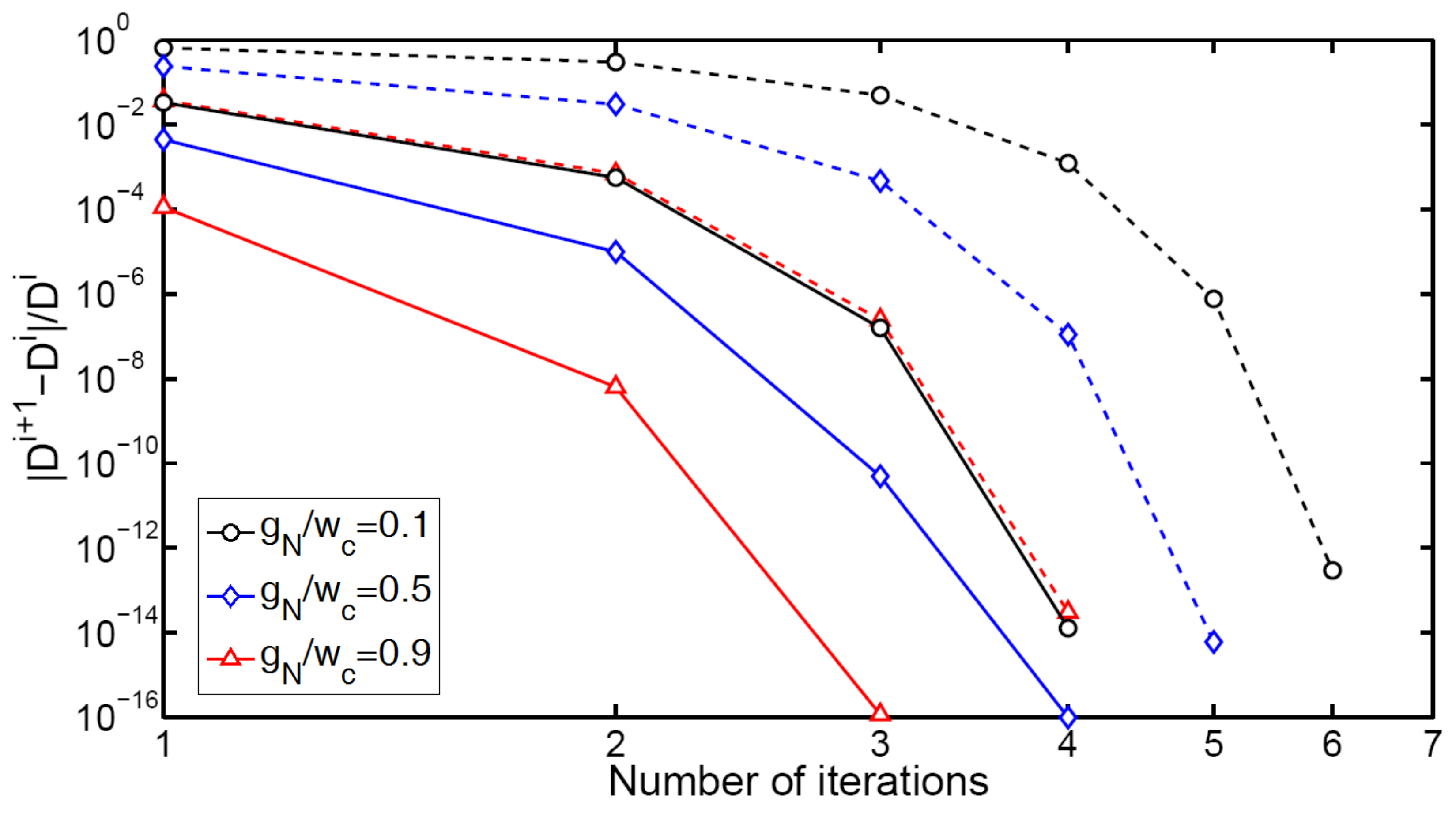

Newton-Raphson loop coupled with an asymptotic expansion solution for the initial values

Application to polycrystalline materials

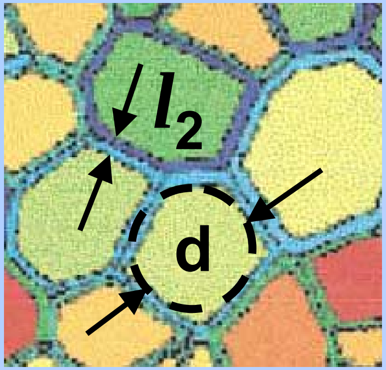

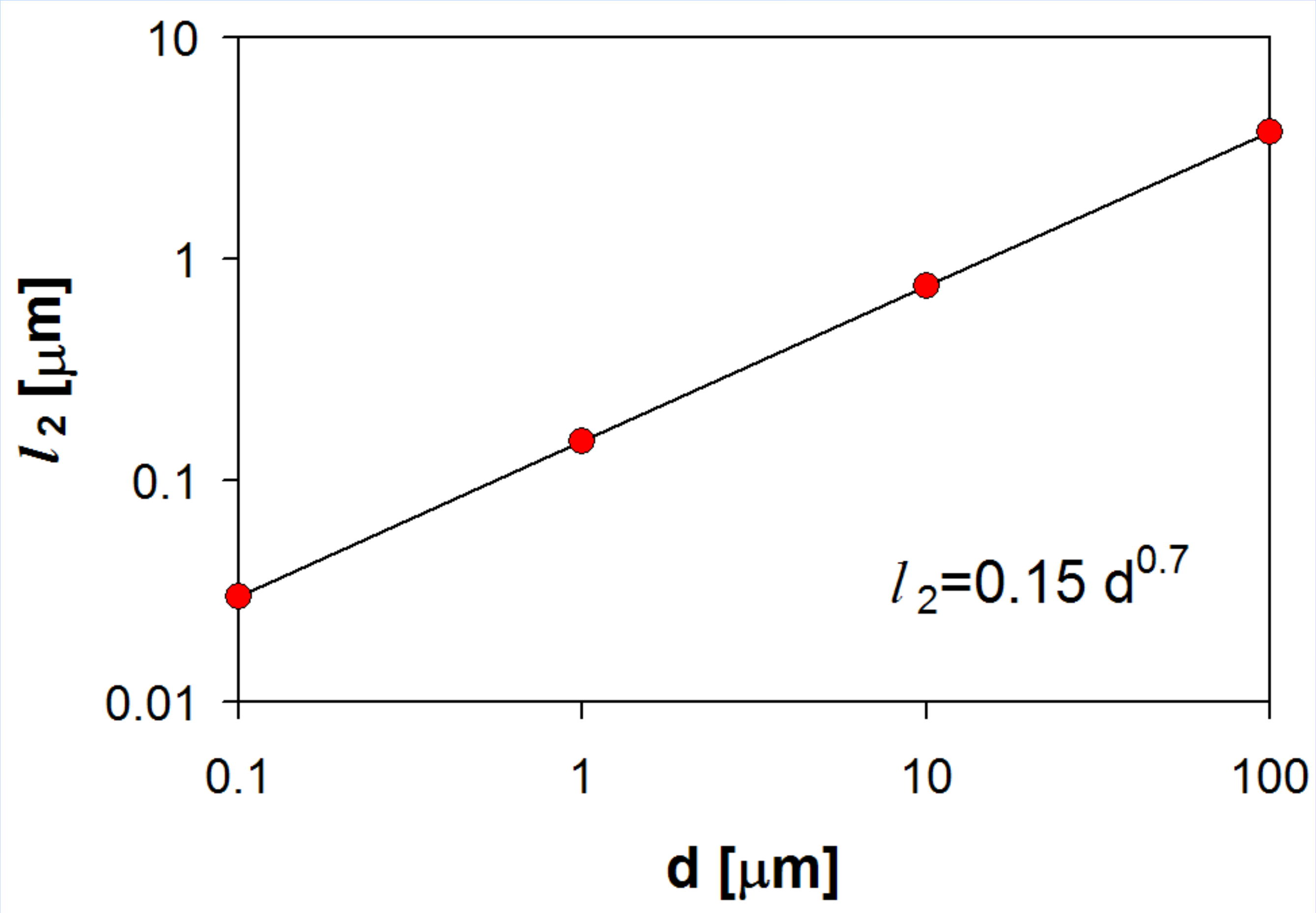

d = grain size

l_2 = interface thickness

Benson et al., **Mat. Sci. Engng.** A 319-321, 854-861, 2001

Application to polycrystalline materials

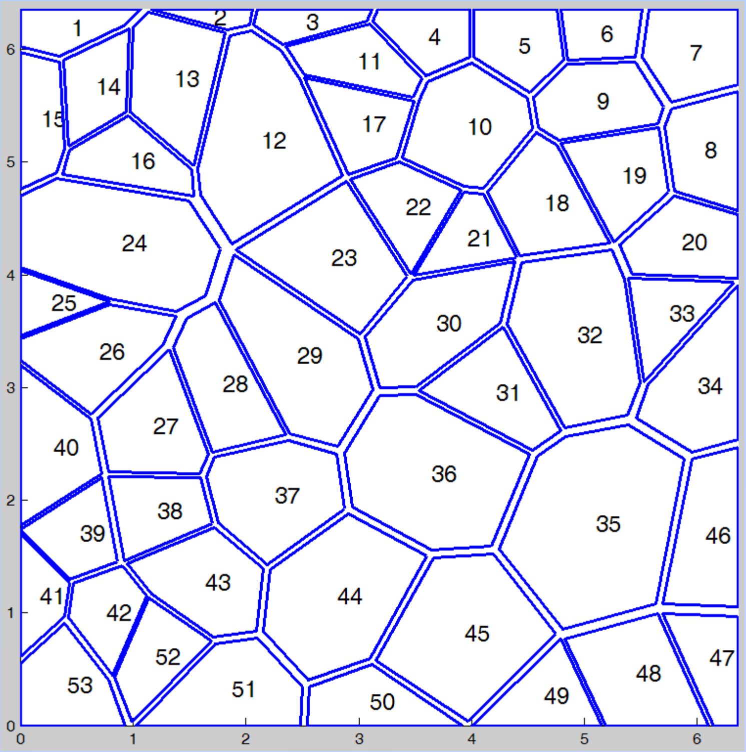

Real microstructure
(Copper)

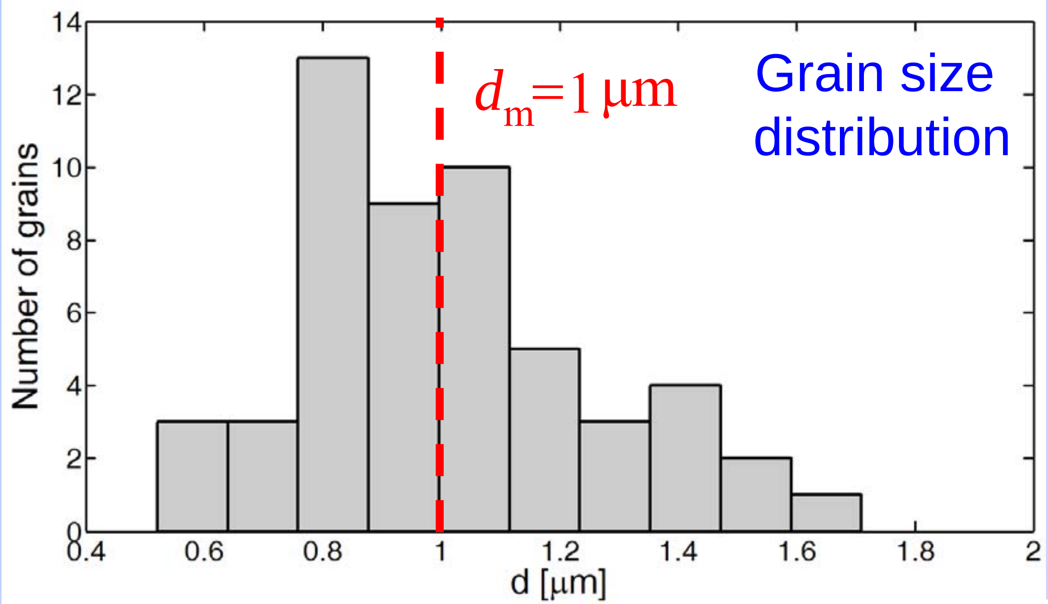

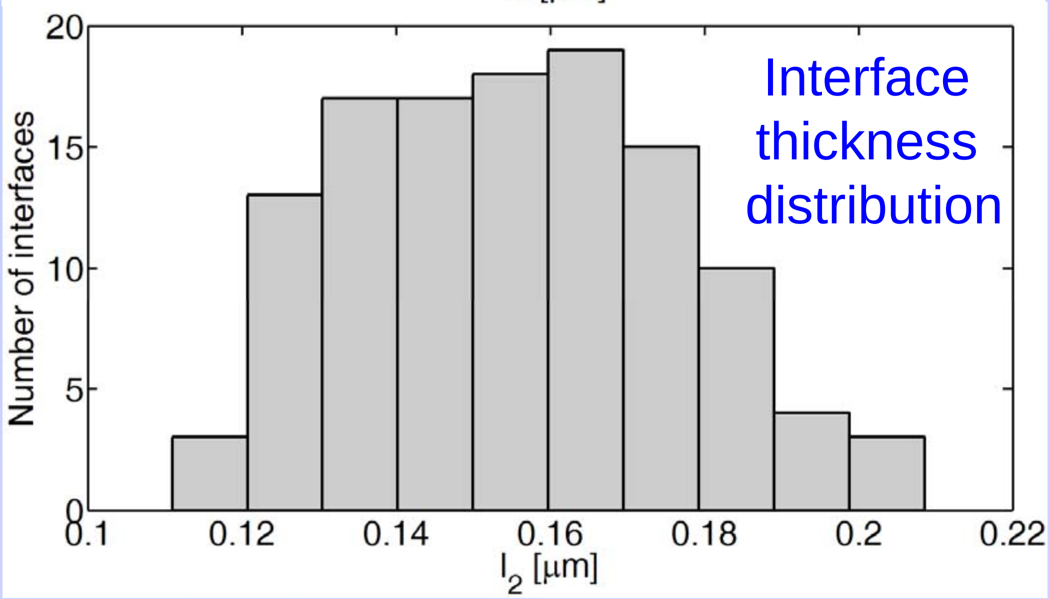

Application to polycrystalline materials

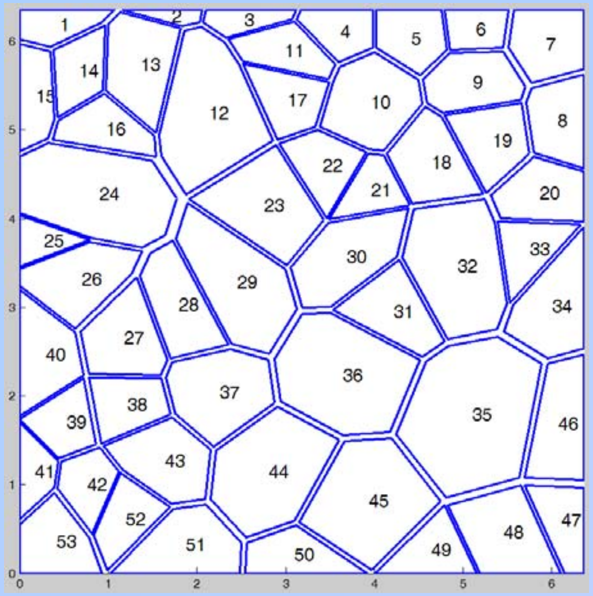

Real material microstructure

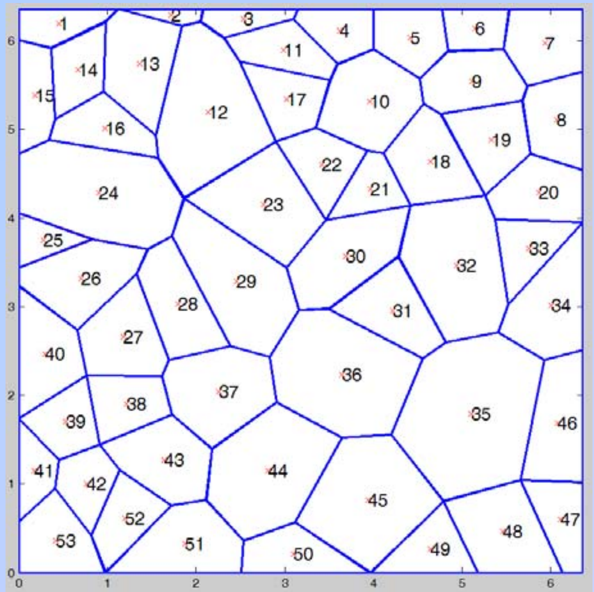

Simplified microstructure with augmented grains & zero-thickness interfaces

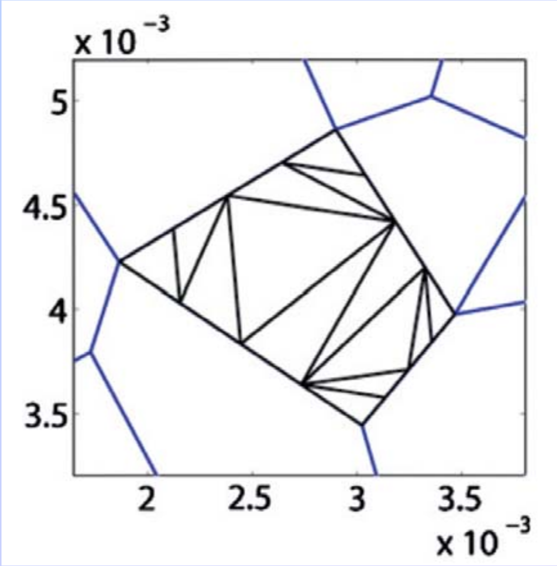

FE mesh with solid & interface elements

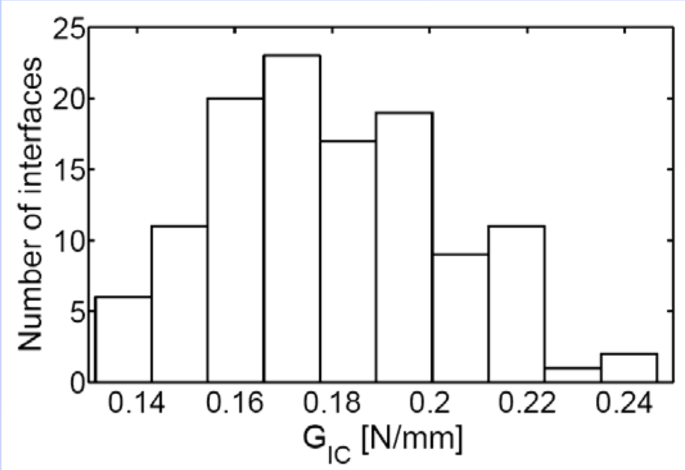

Interface fracture energy distribution

Application to polycrystalline materials

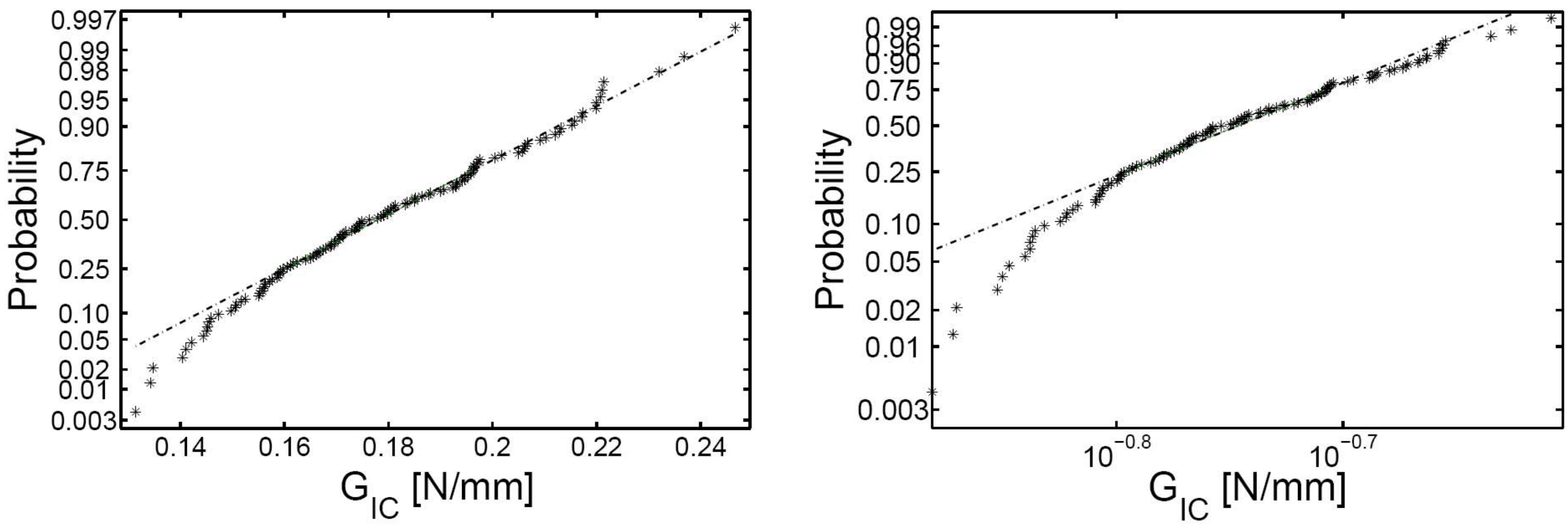

(a) Gaussian probability plot

(b) Weibull probability plot

Comparison with Gaussian and Weibull distributions assumed in stochastic fracture mechanics studies

Simulation of a uniaxial tensile test

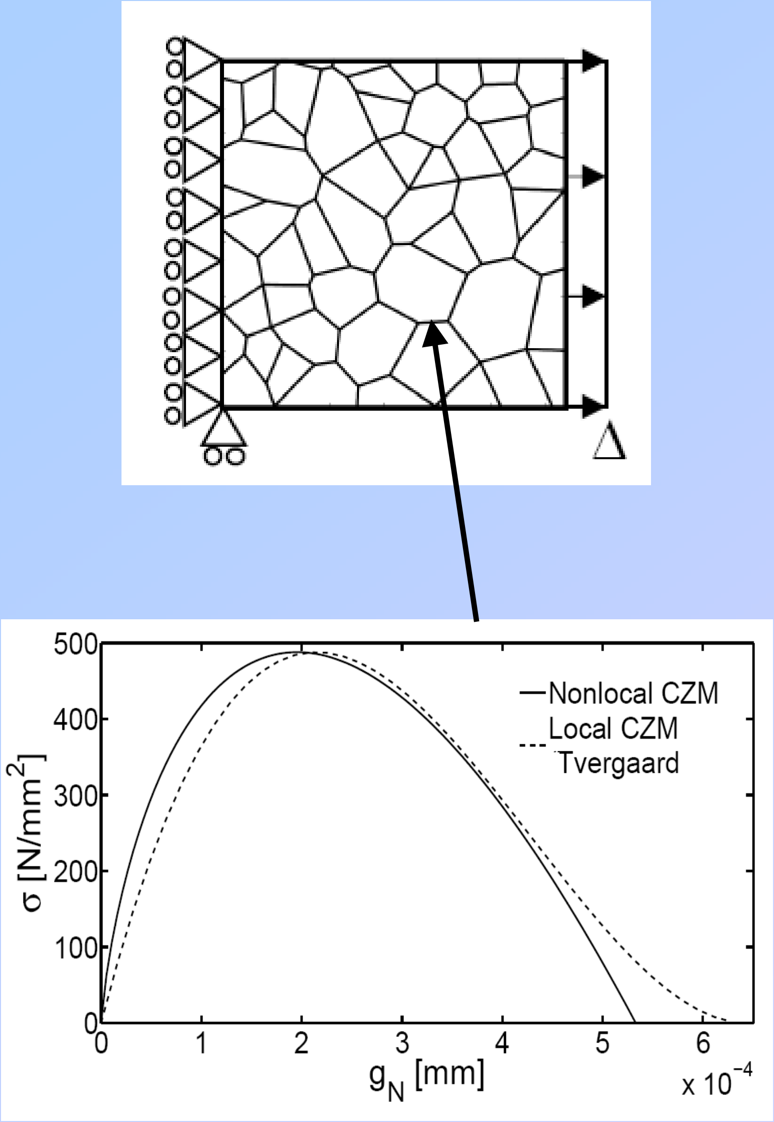

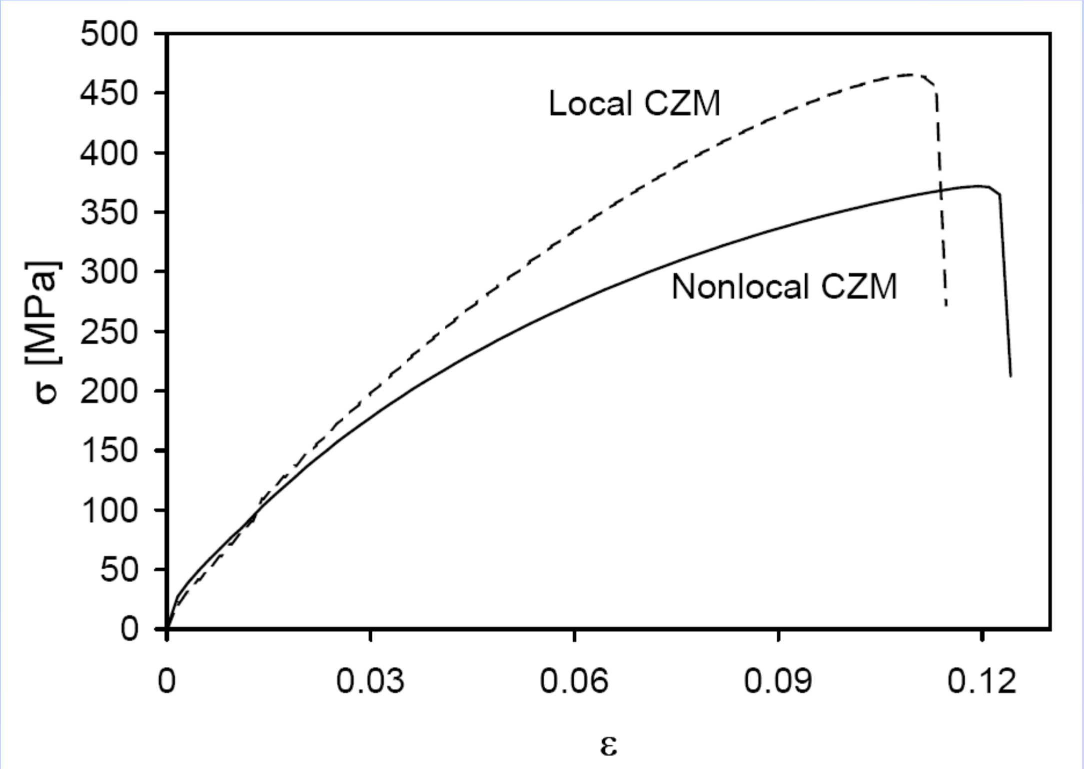

Homogenized stress-strain response

Crack patterns and strain localization

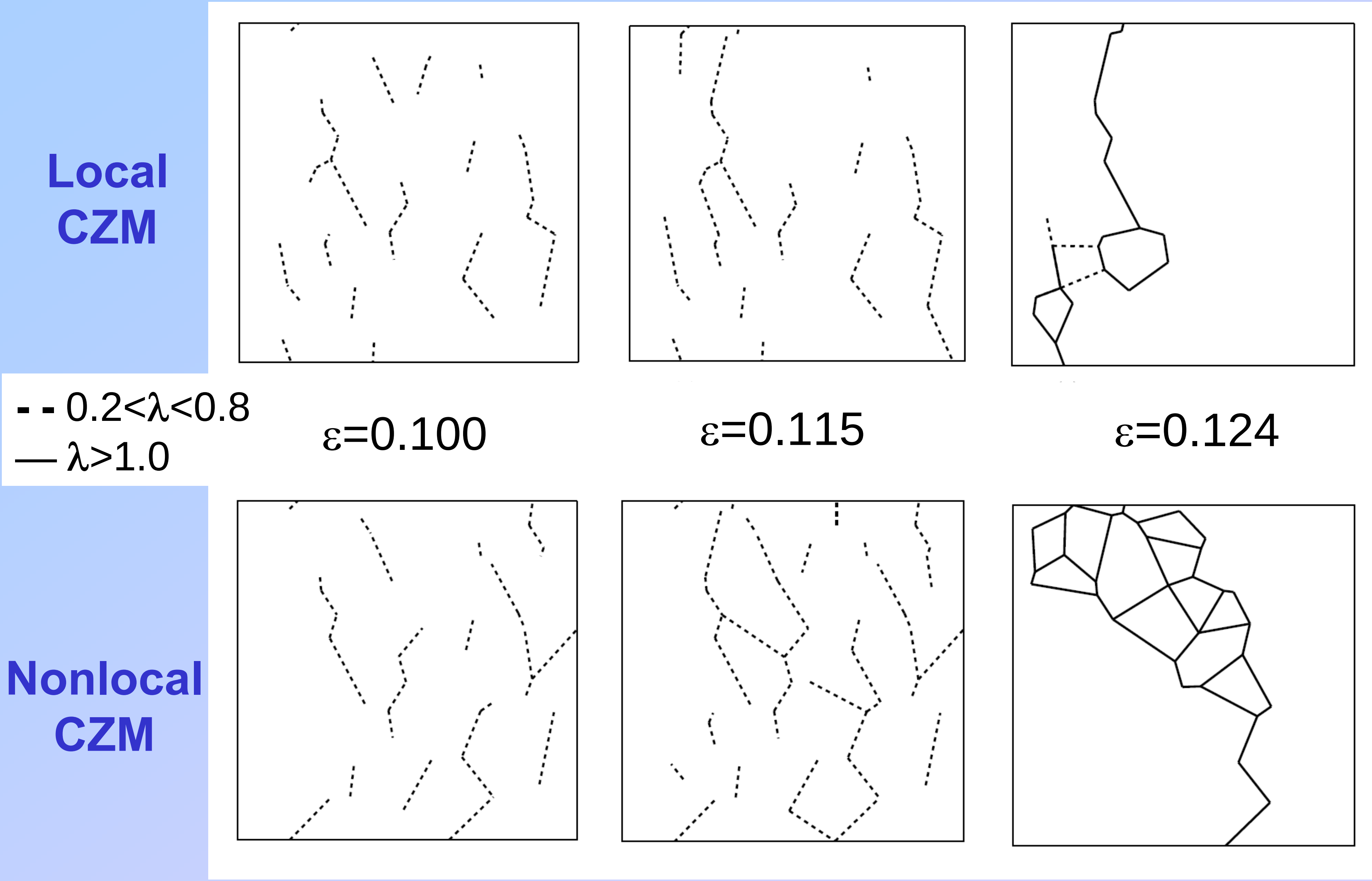

Grain-size effects

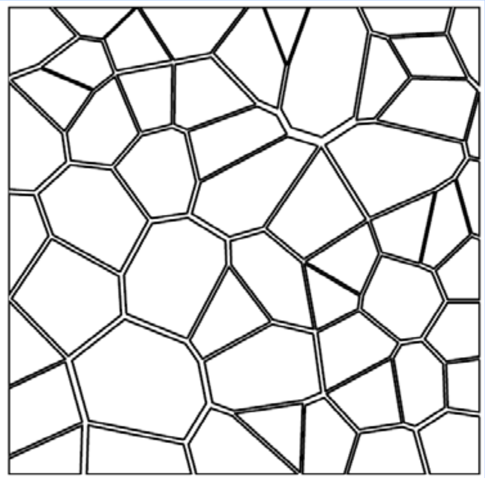

d_m=10 μm

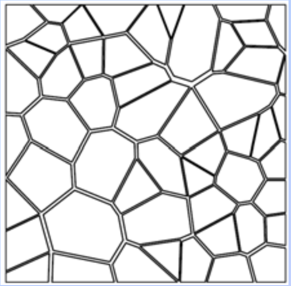

d_m=1 μm

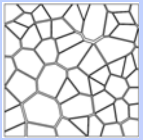

d_m=0.1 μm

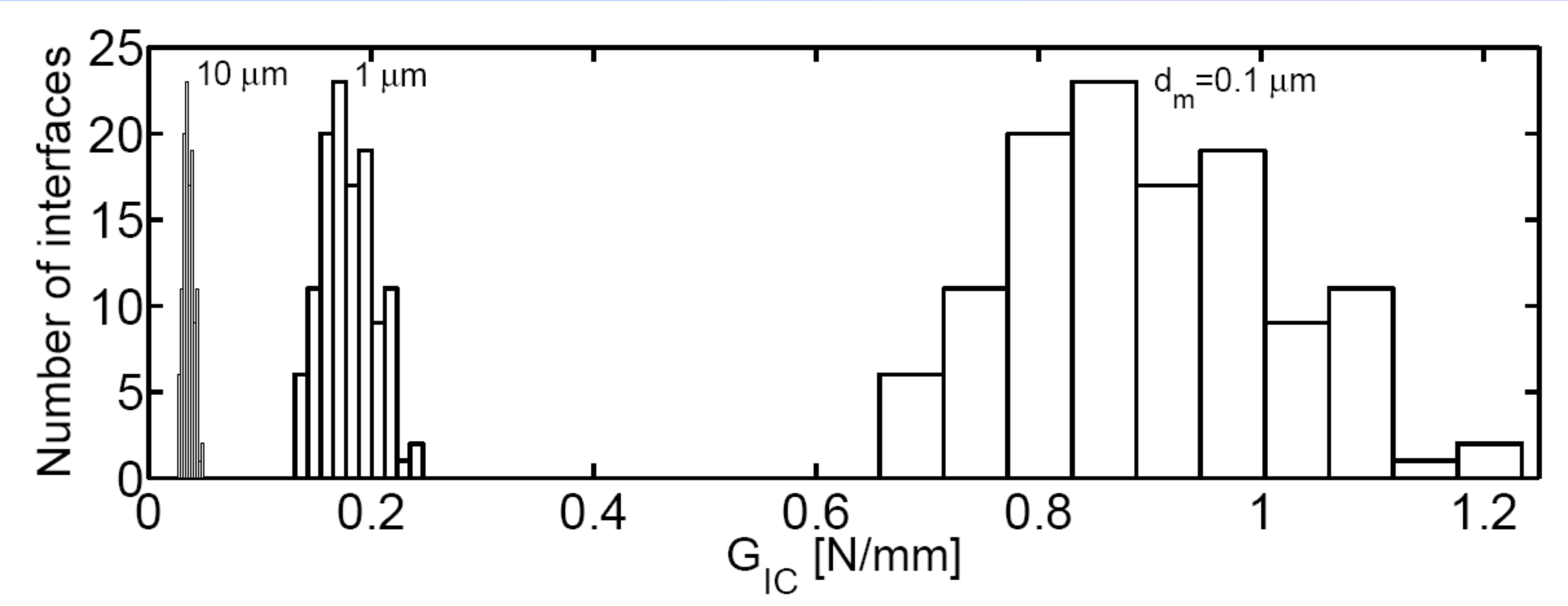

Grain-size effects

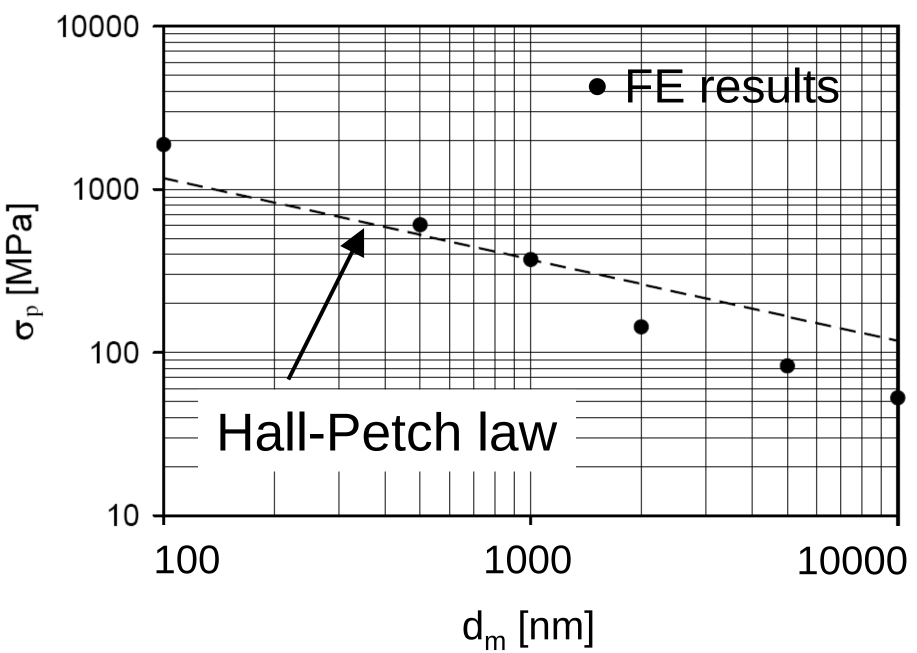

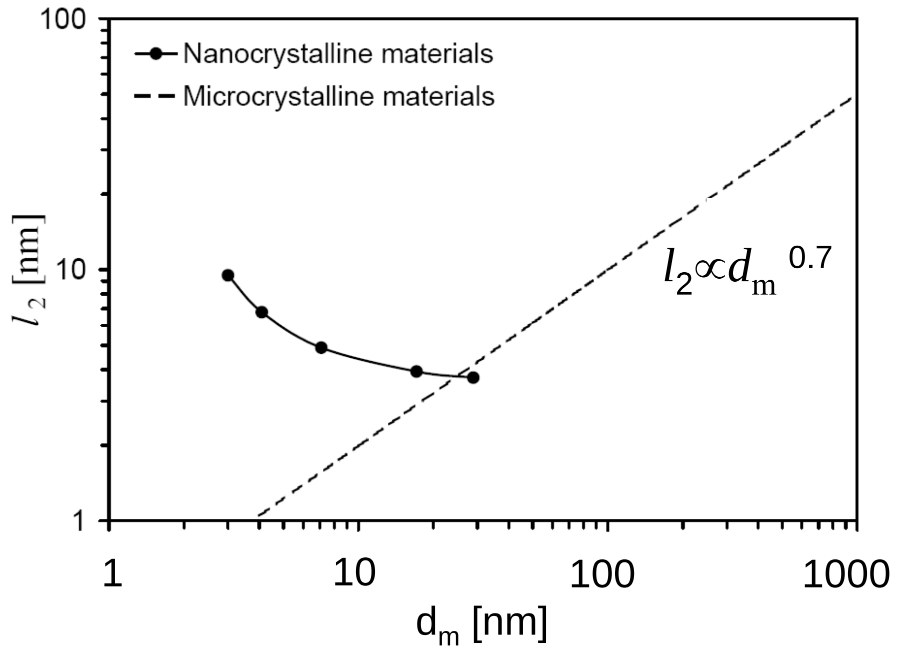

The Hall-Petch law
$\sigma_p \propto d_m^{-1/2}$
is predicted
as a consequence of
$l_2 \propto d_m^{0.7}$

Inversion of the Hall-Petch law at the nanoscale can be the result of the anomalous increase of interface thicknesses

Conclusions

1. A nonlocal CZM based on DM has been proposed for finite thickness interfaces
2. This model overcomes the classical separation between NLFM and DM
3. The parameters of the nonlocal CZM can be related to MD simulations
4. Realistic statistical distributions of NLFM parameters
5. Novel interpretation to the deviation from the Hall-Petch law at the nanoscale

Future developments

3D Modelling of crack propagation in polycrystals and competition between interface decohesion and crystal plasticity

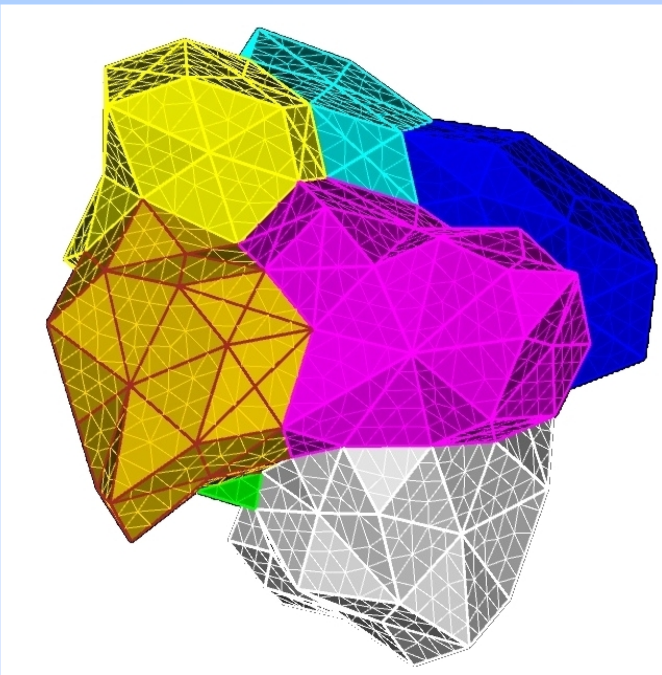

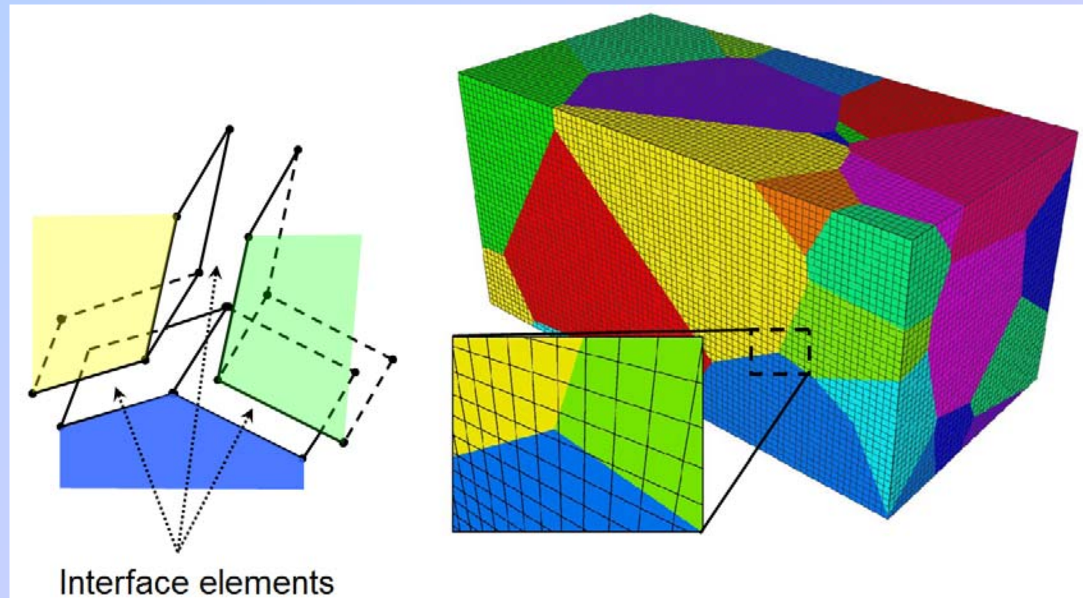

3D image: courtesy of Dipl.-Phys. C. Weber

Vigoni Project 2011-2012 granted by DAAD, MIUR, AIT:
“3D modelling of crack propagation in polycrystalline materials”
Principal Investigators: M. Paggi, P. Wriggers

Acknowledgements

The support of the Alexander von Humboldt Foundation is gratefully acknowledged

Unterstützt von / Supported by

Alexander von Humboldt
Stiftung/Foundation

Special thanks to:

Prof. Dr.-Ing. habil. Peter Wriggers